ADVANCED MATERIALS
www.advmat.de

REVIEW

25th Anniversary Article: Label-Free Electrical Biodetection Using Carbon Nanostructures

Kannan Balasubramanian and Klaus Kern**

Nanostructures are promising candidates for use as active materials for the detection of chemical and biological species, mainly due to the high surface-to-volume ratio and the unique physical properties arising at the nanoscale. Among the various nanostructures, materials comprised of sp^2-carbon enjoy a unique position due to the possibility to readily prepare them in various dimensions ranging from 0D, through 1D to 2D. This review focuses on the use of 1D (carbon nanotubes) and 2D (graphene) carbon nanostructures for the detection of biologically relevant molecules. A key advantage is the possibility to perform the sensing operation without the use of any labels or complex reaction schemes. Along this spirit, various strategies reported for the label-free electrical detection of biomolecules using carbon nanostructures are discussed. With their promise for ultimate sensitivity and the capability to attain high selectivity through controlled chemical functionalization, carbon-based nanobiosensors are expected to open avenues to novel diagnostic tools as well as to obtain new fundamental insight into biomolecular interactions down to the single molecule level.

1. Introduction

Nanostructures can be broadly classified as 0D, 1D and 2D materials.[1,2] 2D nanomaterials refer to structures that are extended in two dimensions, with the size along the third dimension measuring less than 100 nm. The thinnest 2D material realizable today is graphene, which comprises of just a sheet of sp^2-bonded carbon atoms.[3] When one imagines that such a sheet is rolled-up we obtain a single-walled carbon nanotube (CNT), which can be seen as an extended cylinder (a 1D nanostructure) with a diameter typically of the order of 1 nm.[4] Going one level further down, we arrive at fullerenes, which are bucky balls of carbon with a diameter in the range of 1 nm, representative of 0D structures.[5] Due to their high surface-to-volume ratio and reduced surface, the electronic properties of such materials are very sensitive to their environment.[6,7] Added to this, the fact that the sizes of such nanostructures are comparable to that of individual biomolecules has strongly motivated their use for the sensitive detection of chemical and biological species.

Detection of biomolecules is fundamentally important in a number of fields such as environmental analysis, identification of biological threats and in medical diagnosis. Among all these application areas, modern molecular diagnostics has been the driving force for the extensive research on nanoscale biosensors.[8] The current trend in the domain of medical sciences is to investigate the molecular basis of various diseases rather than attempt just a symptomatic treatment.[9] Specific biomarkers are being identified as being the cause for a certain disease or disease state. Typical examples of simple biomarkers range from small molecules through nucleic acids to peptides and proteins that are found in bodily fluids.[10] This paradigm requires the detection of biomarkers directly in physiological fluids, based on which a clear diagnosis of a disease or disease state can be ascertained. The lower the detection limit of a biosensor for a certain biomarker is, the earlier the disease can be diagnosed.[11] In turn, the diagnosis of a disease at an early stage leads in many cases to a simpler and more effective therapy. With their promise of near absolute sensitivity and single molecule detection capability, the use of nanostructure-based sensors raises hopes for opening new avenues in medical diagnosis and the ensuing therapy. Moreover, the ability to detect biomolecules in low concentrations both in vitro and in vivo is expected to provide new insights into the role of various biomarkers in the cause of a specific disease.

The detection protocols or assays that are currently in use achieve a low detection limit by utilizing some preprocessing of the target molecule (analyte) that is to be detected. A typical example is a nucleic acid assay that utilizes an amplification strategy called polymerase chain reaction (PCR) to replicate the target analyte and thereby obtain a high concentration of the same target nucleic acid sequence.[12] However, for proteins no such amplification strategy exists. As a consequence, the possibility to detect very low quantities of a target protein is an important prospect,[13] where the nanostructures appear to provide an unique advantage with respect to currently prevalent detection protocols.

Another important aspect is that most of the currently prevalent protocols are based on optical detection, wherein a fluorescent marker is used to identify the presence of a certain analyte (see **Figure 1**(a)).[14] This requires labeling the

Dr. K. Balasubramanian, Prof. K. Kern
Max Planck Institute for Solid State Research
Heisenbergstrasse 1, D70569, Stuttgart, Germany
E-mail: b.kannan@fkf.mpg.de; k.kern@fkf.mpg.de
Prof. K. Kern
Institut de Physique de la Matière Condensée
Ecole Polytechnique Fédérale de Lausanne
CH1015 Lausanne, Switzerland

DOI: 10.1002/adma.201304912

target analyte directly with a fluorophore or through the use of further reaction steps. These aspects further increase the detection limit attainable in typical assays. Since the presence or absence of just a few analyte molecules in the vicinity of a nanostructure leads to distinct changes in their electrical properties, electrical detection methods show promise to attain very low detection limits.[15,16] Such a strategy does not require any additional labeling of the target molecule or other reaction steps and the analyte can be detected in a straightforward manner (see Figure 1(b)). Here, we will focus only on those examples, where a label-free detection paradigm has been utilized when sensing biomolecules using nanoscale devices based on carbon nanostructures (CNSs). In such a scenario, one or few CNSs constitute the active material of the device, which is prepared in a field-effect configuration. In some cases, the resistance of the device has been utilized as the sensor signal.

The review is organized as follows. We start with a general introduction of carbon nanostructures describing their physical and chemical properties and comparing them in the context of other nanomaterials that are used for the realization of biosensors. Following this, we present the fundamentals of label-free electrical detection discussing the various device architectures and measurement strategies that are currently well-established. In order to obtain selectivity towards a specific target analyte it is necessary to modify the surface of the nanostructure with an appropriate binding partner. (Bio) chemical functionalization protocols intended to achieve this are presented next. Subsequently the sensing mechanisms are analyzed, which are key to understanding the sensor response. Building up on these basics, various sensing protocols for the detection of nucleic acids and proteins are compared. Here we also focus on methods to tune the sensitivity of the realized sensors and the possibility to follow the activity of individual enzyme molecules. We conclude with a discussion about the fundamental limits and future prospects of carbon-based nanobiosensors depicting the key hurdles that are to be overcome for the widespread deployment of such biosensors.

Kannan Balasubramanian is group leader at the Max Planck Institute for Solid State Research in Stuttgart, Germany. His group focuses on the investigation of biomolecular interactions occurring at the nanoscale using carbon-based nanostructures. He obtained his Ph.D in the area of nanostructure physics from the Ecole Polytechnique Fédérale de Lausanne (EPFL), Switzerland in 2005. He completed his habilitation in Analytical Chemistry at the Justus Liebig University of Giessen, Germany in 2012. His research interests include fundamental aspects of solid/liquid interfaces for future device applications in sensing and energy conversion.

Klaus Kern is Director and Scientific Member at the Max Planck Institute for Solid State Research in Stuttgart, Germany, Professor of Physics at the Ecole Polytechnique Fédérale de Lausanne (EPFL), Switzerland, and Honorary Professor at the University of Konstanz, Germany. His present research interests are in nanoscale science, self-ordering phenomena and chemistry and physics of surfaces and interfaces. He holds a chemistry degree and PhD from the University of Bonn. After his doctoral studies he was staff scientist at the Research Center Jülich and visiting scientist at Bell Laboratories, Murray Hill before joining the Faculty of EPFL in 1991 and the Max- Planck-Society in 1998.

2. Carbon Nanostructures

In this section, we first outline the various methods for the synthesis of carbon nanostructures. Broadly speaking decomposing a carbon source at a high temperature (>900°C) in the presence of a transition metal catalyst leads to the formation of sp^2-bonded carbon structures. This growth method is termed chemical vapor deposition (CVD). The underlying form of the catalyst dictates the kind of nanostructure obtained – CNTs grow from nanoparticles, while with a metal film we obtain graphene. However, there are other methods, which are specific to CNTs or graphene, as discussed below. In order to realize sensors, the nanostructures have to be positioned on a substrate. Various strategies to position such nanostructures on silicon or glass substrates are presented next. Following this, we compare the physical and chemical properties and analyze the pros and cons of carbon nanostructures over other nanostructured materials for biodetection.

2.1. Carbon Nanotubes

Carbon nanotubes can be visualized as cylinders obtained by rolling up individual layers of graphite as shown in **Figure 2**. Depending on the orientation of the tube axis with respect to the hexagonal lattice, we obtain different chiral forms termed as armchair, zigzag or chiral.[17] The growth of CNTs can be performed using various methods such as arc discharge,[18] laser ablation,[19] chemical vapor deposition (CVD)[20] or high pressure pyrolysis of carbon monoxide.[21] While many research activities focus on controlling the diameter of the tubes during growth, until today there is no method available with which CNTs of a specific chiral form can be specifically grown.[22] Another interesting aspect with CNTs is that their electrical properties differ depending on the chiral form of the tube – they can be metallic, semi-metallic or semiconducting.[23] A metallic

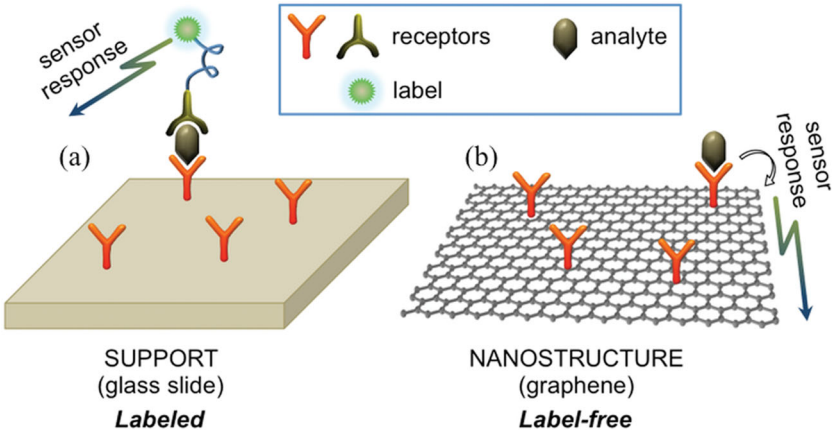

Figure 1. Simplified schematic showing the key aspects of (a) labeled and (b) label-free detection schemes on surfaces. In both cases primary receptors are first immobilized on a support or on the nanostructure surface. In the case of label-free detection (b), the binding of the analyte molecule to the receptor directly induces changes in the physical properties of the underlying nanostructure. In labeled detection schemes (a), the bound analyte is detected through further reaction steps with the help of a label (e.g., fluorescent or radioactive). In the example shown here, a secondary receptor with an appropriate label binds to the free end of the analyte and generates a sensor response.

CNT is characterized by a constant density of states around the Fermi level, while semiconducting tubes exhibit a band gap whose value is approximately given by 0.7 eV/d, where d is the diameter of the nanotube in nm.[24] CNTs with larger diameters are mostly semi-metallic due to a much smaller band gap. The non-availability of one specific chiral form and the presence of different electrical properties in the same sooth of CNT raw material have been the major drawbacks for the widespread use of CNTs in various applications. In order to obtain a single or few chiral forms, some kind of post-processing is necessary, such as gel filtration, chromatography or ultra-centrifugation.[22] Based on these strategies, it is now possible to obtain carbon nanotubes with a limited subset of chiral forms, which can also be commercially procured as dispersions.[25]

In order to realize devices, the CNTs have to be deposited on a substrate such as silicon or glass. All the reported methods for depositing CNTs can be classified under bottom-up or top-down approaches. In the bottom-up approach, catalyst particles acting as growth seeds are deposited on an appropriate substrate and the tubes are grown using CVD.[26] In order to contact the nanotubes, a subsequent lithography step is used to pattern electrodes.[27] Alternatively, the patterning of electrodes as well as the catalyst can be done before growth, in order to obtain CNTs at predefined locations.[28] Although this approach sounds very versatile, it is difficult to obtain a homogeneous coverage of CNTs on a large scale, leave alone the fact that there is a variation in the electronic properties of the obtained CNTs.[29] In top-down approaches, the CNTs are dispersed in aqueous or organic solvents and subsequently deposited on to the substrate.[22] Typically, one has to locate the CNTs on the substrate in order to contact them. This is usually done with the help of serial techniques such as Atomic Force Microscopy (AFM) for locating the tubes and electron beam lithography (EBL) for contacting them.[30,31] Despite the cumbersome nature of this method, many sensors have been successfully demonstrated using this strategy.[32,33] One way to overcome the drawback of serial processing is to utilize directed positioning methods such as AC dielectrophoresis.[34] Combining this with scalable photolithography methods, we have demonstrated the fabrication of sensors with a high device yield.[35] The advantage here is that almost all of the devices exhibit semi-metallic behavior with low resistances, which are beneficial for the realization of sensors and for obtaining a reproducible sensor response. Typical CNT devices used for sensing are shown in **Figure 3**.

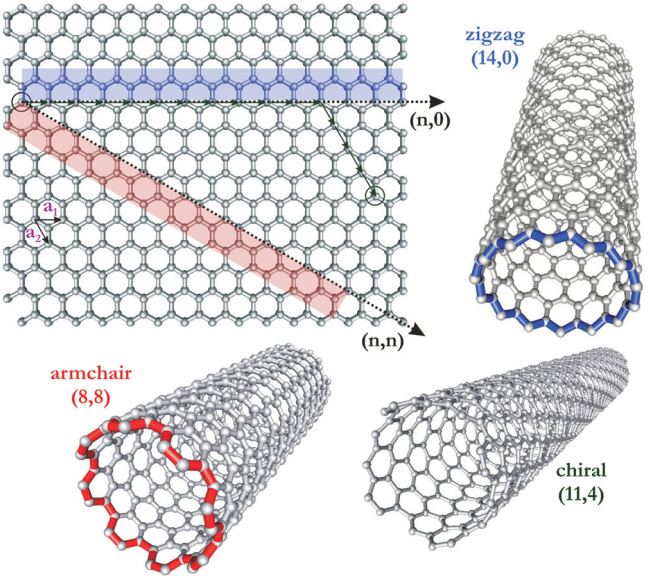

Figure 2. Physical structure of carbon nanostructures. Graphene is an atomic layer of graphite comprised of an hexagonal lattice of sp^2-bonded carbon atoms. Carbon nanotubes are obtained by rolling up a graphene sheet. The roll-up angle with respect to the axis of the tubes determines the type of the tube as zig-zag, armchair or chiral. Reproduced with permission.[17] Copyright 2005, Wiley-VCH.

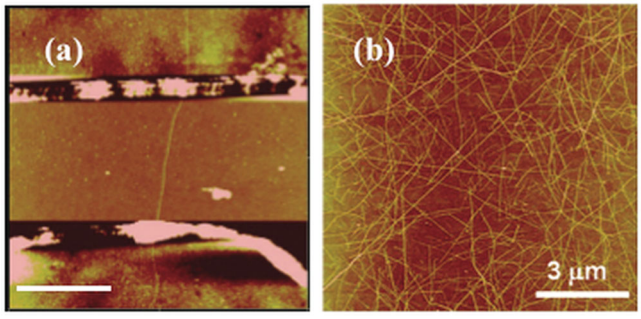

Figure 3. Atomic Force Microscopy (AFM) images of typical field-effect sensors based on carbon nanotubes. (a) Single CNT device (b) CNT network device. *(a)* Reproduced with permission.[33] Copyright 2009, ACS.

2.2. Graphene

The production methods[36,37] reported for graphene can also be classified under top-down and bottom-up approaches. Top-down approaches start with some form of graphite, which is subsequently physically or chemically processed to obtain individual monolayers. In graphite, the individual graphene layers are loosely bound by van der Waals interactions. Hence individual layers can be peeled off by exfoliation or mild agitation in an appropriate solvent.[36] For mechanical exfoliation, typically highly oriented pyrolytic graphite (HOPG) is utilized.[38] The transfer on to a desired substrate is done using a scotch tape.[39] Such crystals are prepared by high temperature pyrolysis and subsequent annealing at around 3000°C, which renders a high degree of crystallinity to the material.[40] Hence, graphene flakes transferred using this method possess very low disorder. Accordingly, mobility values more than 100 000 cm^2/Vs have been observed on exfoliated graphene, depending on the substrate underneath.[41–43] Chemical methods utilize micron-sized graphitic particles as the starting material followed by dispersion in aqueous or organic solvents with or without a surfactant.[44,45] This is analogous to the preparation of CNT dispersions outlined earlier. A disadvantage with such exfoliation methods is that the proportion of monolayers in the dispersion is not very high, although it is possible to obtain a very high concentration of multilayer (less than 5 layers) flakes.

A smart strategy to overcome this disadvantage is based on Hummers method,[46] wherein the graphitic particles are oxidized in a first step using strong oxidizing agents leading to the introduction of oxygen containing groups (hydroxyl, epoxide and carboxyl) in the interstices of the crystal.[47,48] Under controlled conditions, the oxidation can be efficient enough to obtain a high density of monolayer flakes with a second gentle sonication step. Typically these flakes are directly suspended just in water. The presence of negatively charged moieties on the graphene surface prevents the individual layers from aggregation. The price one pays for this efficient exfoliation is that a subsequent chemical processing step is necessary in order to remove the various oxygen-containing functionalities created on the graphene surface. A number of protocols have been reported to perform this reduction, such as thermal annealing,[49] plasma treatment,[47] use of various reducing agents[50] and electrochemical treatment.[51] The reduction itself may be carried out in solution or after transfer on to the final support. Although the resulting electrical properties are graphene-like, they are much inferior in comparison to that of pristine graphene.[47] For example, the mobility is typically much lower than 1000 cm^2/Vs. Microscopic analysis of chemically derived graphene (CDG) or reduced graphene oxide (RGO) has shown that it is comprised of islands of regular graphene interspersed with defective areas.[52] Neveretheless, a number of sensors have been demonstrated by using this strategy.[53–56] This is due to the fact that oxygen-containing groups can be used as anchors to position the graphene flakes on the substrate[53] or as handles for chemical functionalization with biomolecules.[57]

In bottom-up approaches graphene films are directly synthesized either using CVD on metal films or through epitaxial growth on silicon carbide.[36,37,58–60] Typically, one obtains monolayers over large areas using such methods. However, it is difficult to completely exclude rare occurrence of multilayers and amorphous carbon, especially when the synthesis is performed on larger substrates.[61] In both cases, graphene grows in domains and there is a high probability for the occurrence of defects.[62] Typical growth temperatures are in the range of 900–1200 °C. Unlike HOPG, no post-annealing treatment is used, suggesting a comparatively less degree of crystallinity. Nevertheless, the electrical characteristics approach that of mechanically exfoliated graphene with mobility values typically in the range of 1000 to 10000 cm^2/Vs.[37,59] Higher values of more than 10000 cm^2/Vs have also been observed when utilizing a substrate with a low density of defects (such as boron nitride).[63,64] For sensor applications, a lower mobility in general does not represent any disadvantage.

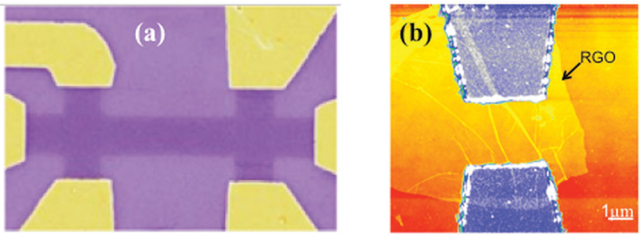

Figure 4. AFM images of typical field-effect sensors based on graphene. (a) mechanically exfoliated graphene (b) reduced graphene oxide (RGO). Reproduced with permission.[43] Copyright 2007, NPG and[53] Copyright 2012, ACS.

In order to realize devices based on bottom-up grown graphene, several transfer methods have been proposed. Generally, it involves the use of a polymer coating on the graphene film followed by etching of the underlying metal.[59] The polymer-supported graphene usually swims in the etching solution, which can be fished out directly using the desired substrate. Various polymers and polymer combinations have been reported, the most common of them being (poly)methylmethacrylate (PMMA) and (poly)dimethylsiloxane (PDMS).[65,66] In order to avoid polymer residues, the use of intermediary layers has also been proposed.[67] Typical examples of graphene devices are shown in **Figure 4**.

The overwhelming interest in the use of graphene is due to the specialized nature of electrical properties exhibited by this material.[59,68] Graphene has a very high conductivity similar to a metal; however, it is a semiconductor with a zero band gap.[69] The electrical nature of graphene is similar to that of semimetallic CNTs, which have a very small band gap (<50 meV). Due to this aspect, the electronic transport in graphene exhibits an ambipolar behavior, in the sense that both hole and electron transport can be observed in a small energy range. For device applications, the possibility to have both holes and electrons opens up new device concepts that can help improve the performance of such devices.[70,71]

2.3. Physical and Chemical Properties

Before we proceed to discuss the various biodetection paradigms it is worth shedding light on the physical and chemical properties of the two kinds of nanostructures. Both CNTs and

graphene comprise of an extended pi-conjugated network, which is key for the characteristic electrical properties. As mentioned above, CNTs come in a variety of forms, with their electronic properties ranging from metallic through semi-metallic to semiconducting. On the other hand, graphene almost always exhibits a semi-metallic behavior. Efforts are underway to introduce a band gap in graphene, however, no reliable method is yet available for performing this in a persistent manner, without disturbing the underlying graphene electronic structure significantly. One possibility is the further structuring of graphene to obtain nanoribbons that are less than 20 nm in width, where transport gaps have been observed. However, it is still a tedious procedure to obtain such nanoribbons and there is no report yet on the use of such nanoribbons for biodetection. Typical sensors made using graphene have channel widths in the range of 100 nm to 1 micron. By comparison, the channel width of an individual nanotube device measures around a nanometer, and that of bundle devices extend a few nm. The lengths of both kinds of devices range from a few 100 nanometers to a few microns. It is apparent that the effective surface area is orders of magnitude smaller for nanotubes in comparison to that of graphene. Both CNT and graphene devices have been shown to exhibit high carrier mobilities, which can be attributed to the highly correlated carrier distribution in 1D and 2D systems that reduces back scattering significantly.[41]

An important difference between the two types of nanostructures arises due to their nature being 1D or 2D. This leads to a differing electronic structure as shown in **Figure 5**. CNTs are characterized by predominant van Hove singularities both for metallic and semiconducting tubes,[72] while graphene shows a linear dispersion relation around the charge neutrality point.[3] Moreover, the effective density of states around the Fermi is much lower for nanotubes. As a result, nanotubes exhibit high capacitances for charging or filling of the energy levels.[73,74] This quantum capacitance is much lower for micron-sized graphene flakes.[75,76] These fundamental differences in electronic structure are also pivotal for the ensuing electrical characteristics, especially when charge transfer or charge modulations take place at the surface of such nanostructures in liquid. Furthermore, the diffusion profile is radial for nanotube devices while planar for graphene. In general, the diffusion is slightly stronger with a radial rather than with a planar profile.[77]

An intact pristine CNT has sp^2-bonded carbon all along the body of the cylinder. Although the edges may be open or closed with an appropriate fullerene, in most of the transport measurements the ends do not play much of a role. In contrast, graphene flakes contain edges, where localized states exist analogous to surface states in a bulk material. While many reports show that the electronic structure at the edges may have a considerable impact on the device characteristics,[58,78,79] they have not yet been shown to play a dominant role in the sensing characteristics of the fabricated devices.[80,81]

There are distinct differences in the chemical nature of these two types of nanostructures as well. Since the reactivity of sp^2-carbon can be considered to be rather low, drastic reaction conditions are necessary to obtain consistent chemical modification on the pristine graphene surface.[17,82–84] However, CNTs are expected to show a comparatively higher reactivity due to their curvature. Moreover, defects, vacancies and catalyst

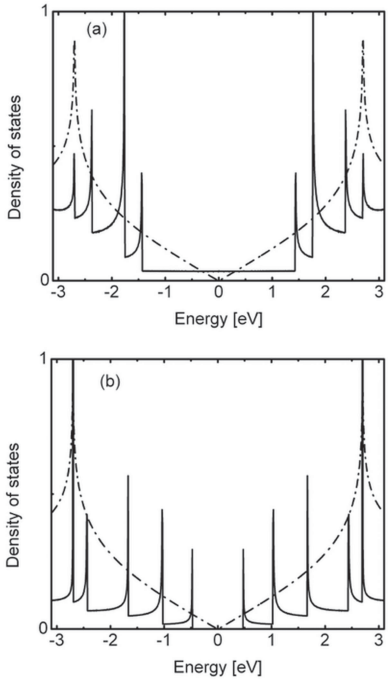

Figure 5. Electronic structure of carbon nanostructures. Electronic density of states (DOS) for (a) metallic (9,0) CNT and (b) semiconducting (10,0) CNT at 0K. In both the graphs, the dash-dotted line shows the DOS for graphene. Characteristic van Hove singularities due to the quasi 1D nature of CNTs are apparent, while graphene exhibits a linear density of states close to the Fermi level. In (a) the DOS is low around the Fermi rendering the (9,0) CNT with a quasi-metallic behavior. Around the Fermi level, the DOS is zero for the (10,0) CNT. The DOS is zero at the Fermi level for graphene, however with a zero band gap. The data were obtained using a tight binding model with a tight binding integral of –2.7 eV.

centers along the sp^2-bonded carbon framework contribute in general to an increased reactivity.[17,85,86] Graphene has basal plane sites similar to the surface of HOPG and edge plane sites with dangling bonds. It has been reported that the edge plane sites are more reactive in comparison to the basal plane sites.[87] Hence it can be expected that the reaction be easily initiated at the edges. However, there is no consistent report of achieving such a controlled functionalization on exfoliated graphene yet. On chemically derived graphene, it has been proposed that the reaction takes place predominantly at the defect sites, however there is no microscopic proof confirming this.[81] Moreover, recent local electrochemical studies suggest that the difference in reactivity between basal and edge plane is not that prominent.[88] From the foregoing discussion, it is apparent that the chemical reactivity of carbon nanostructures is still a matter of intense research, where a number of open questions still remain.

2.4. Comparsion with Other Nanostructures

The use of nanostructures for label-free electrical biodetection is still in a research stage. Hence, it is difficult to identify the best-suited material in this field. However, it is worthwhile

comparing the pros and cons of carbon nanostructures against others. Among them inorganic nanowires constitute an important class of materials,[89,90] of which silicon nanowires represent the majority.[91] One of the major reasons for the success of silicon nanowire devices is that many of the processes required to fabricate them are already available as part of the microelectronics industry. This allows for a controlled engineering of these structures with the possibility to readily tune their electronic structure through variations in composition or doping.[15,92] A plethora of biosensors have been demonstrated for the detection of various biomolecules using silicon nanowire-based devices.[15,92] Unlike CNTs, arrays of SiNWs can be fabricated in a facile manner,[93,94] thereby allowing for the multiplex detection of more than one analyte.[95] There is only one example of such a demonstration with CNTs for the detection of gases.[96]

On the other hand, there are specific advantages of using carbon nanostructures for biodetection. The rich carbon-based chemistry paves way for the easy design of a broad range of functionalization protocols that is compatible with standard biodetection protocols. Further, passivation of such surfaces is not necessary, even in extreme conditions (such as highly basic or acidic or in organic solvents). By contrast, almost all of the functionalization methods for SiNWs reported until now are based on the use of silanes.[97] Moreover, a native silicon oxide layer is typically present in most devices, which in some cases may limit the intrinsic performance of such devices.[98] Another important difference is that the resistances of CNT and graphene devices are in the low kiloohm range, while that of inorganic nanowires are generally in the low megaoohm range. This reduces noise in carbon-based devices considerably and favors a faster sensor response due to a low RC time constant. In spite of these advantages a number of drawbacks still persist. With silicon nanowires it is rather straightforward to obtain wafer-scale devices with reproducible electrical characteristics. While this appears feasible when using transferred CVD graphene, there is no universal method to obtain CNT devices in high throughput with homogeneous electrical characteristics. This imposes serious limitations for the calibration of the sensors that is mandatory for e.g for on-site applications.

3. Fundamentals of Label-Free Electrical Detection

3.1. Basic Concept

The fundamental concept behind the use of a label-free paradigm is based on the detection of a binding event occurring on the surface of a nanostructure leading to a direct change in its physical properties. The possibility to perceive this change is unique for the case of nanostructures, due to the miniaturized size and the high surface-to-volume ratio. A generalized picture of an ideal label-free electrical sensor is shown in **Figure 6**. In order to realize the binding event, an appropriate binding partner (called the receptor) is immobilized on the nanostructure surface. The receptor is chosen in such a way that it exclusively binds to or interacts with the target bimoloecule (analyte) of interest. For example, to detect a specific nucleotide

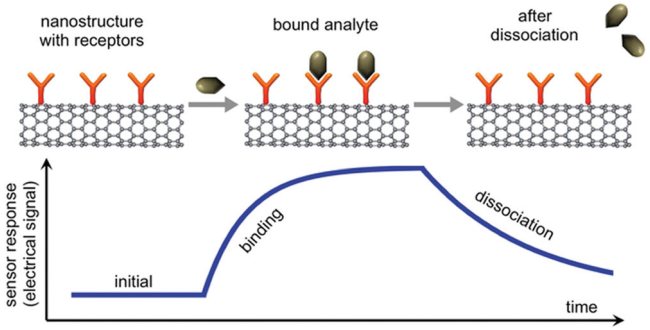

Figure 6. General concept of label-free electrical detection using carbon nanostructures in an ideal situation. In a first step, a receptor specific to the target molecule (analyte) is immobilized on the nanostructure surface. The electrical properties of the nanostructure such as resistance or field-effect behavior is monitored as a function of time. The binding of the analyte leads to variations in these electrical characteristics, which can be detected through the measurement signal. If the binding is reversible, the initial characteristics can be recovered.

sequence, the corresponding complementary sequence can be utilized. This is a critical aspect in the design of the sensor, since the receptor is the key component that brings selectivity to the detector. Addition of a solution containing the analyte molecules leads to the binding of these molecules on to the functionalized sensor surface. The binding process itself is governed by the kinetics of the binding reaction under investigation. In most of the sensors discussed here the time required to reach steady state at saturation is in the order of few minutes to a couple of hours. The binding event is expected to alter the charge distribution on the surface and thereby affect the electrical properties. These changes are registered by measuring for e.g., the resistance of the underlying nanostructure. In the event of the binding being reversible, the original situation can be recovered through appropriate changes in the reaction conditions. In the following, we discuss various technical aspects related to the detection paradigms and measurement strategies. Following this, we focus on selectivity issues by presenting bio/chemical functionalization protocols that have been reported to attach a broad range of receptors to the nanostructure surface. Finally, we turn to the sensing mechanisms that play a major role in the initiation of the sensor response.

3.2. Device Architectures and Measurement Strategies

The simplest sensing strategy is to measure the electrical resistance of a nanostructure (or a nanostructure ensemble) in the dry state before and after the binding event takes place on its surface. Strictly speaking, however, the interfacial charge distribution couples in most cases capacitively with the underlying nanostructure. As a result, a field-effect transistor (FET) configuration (**Figure 7**) is more beneficial to measure the sensor response. For this purpose, the devices are fabricated on highly doped silicon substrates with a thermally grown oxide layer (few 100 nm in thickness). The highly doped silicon serves as the gate, while the oxide functions as the gate insulator in a 'back-gated' configuration as shown in Figure 7(a). This configuration

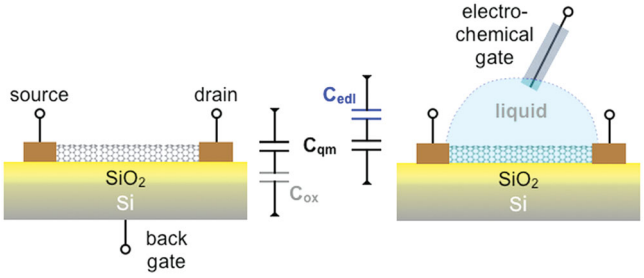

Figure 7. Schematic diagram showing the two different field-effect detection paradigms. (a) back-gated configuration and (b) liquid-gated configuration. The resistance of the carbon nanostructure across the source-drain contacts is measured as a function of the gate voltage. In (a) the gate insulator is provided by the oxide layer present on the substrate. In (b), the electrical double layer at the CNS-liquid interface serves as the gate insulator. The gate electrode in (a) is the underlying highly doped silicon substrate. In (b) a reference electrode such as a Ag/AgCl wire is used as the gate electrode. The geometrical capacitance in (a) is given by the oxide capacitance (C_{ox}), and in (b) by the capacitance of the electrical double layer (C_{edl}). The quantum capacitance (C_{qm}) of graphene or CNT appears in series with the geometric capacitance.

is prone to hysteresis due to the presence of charge traps from water molecules in the gate insulator.[99] The hysteresis can be overcome to a great extent by carrying out the measurements directly in solution, referred to as 'liquid-gated' or 'electrochemically gated' configuration as shown in Figure 7(b).[74] In such a situation, the capacitive coupling from the binding event takes place through the electrical double layer formed at the nanostructure/solution interface.[74] The potential of the nanostructure channel is adjusted with the help of a reference electrode (working as the gate) that is kept in contact with the solution, as is common in experiments in the field of electrochemistry. This arrangement is very similar to the ion-selective field-effect transistor (ISFET) [100] that is commonly used for example to design pH electrodes. The choice of the reference electrode has also been found to have a crucial impact on the sensor response.[101,102]

In a field-effect configuration, the gate capacitance plays a key role in the observed device characteristics.[103] Two capacitances appear in series namely the geometric capacitance (C_{geo}) and the quantum capacitance (C_{qm}) as shown in the Figure 7. C_{geo} represents the oxide capacitance (C_{ox}) for the back-gated configuration and the double layer capacitance (C_{edl}) for the liquid-gated configuration. C_{geo} is cylindrical for the nanotube and planar for graphene (similar to a parallel plate capacitor). In a back-gated configuration, the geometric capacitance dominates the FET characteristics.[74,103] C_{qm} becomes important when using the liquid-gated configuration. For solutions with ionic strength lower than 100mM, the double layer capacitance is at least 14 pF/cm for an individual CNT and increases as the ionic strength goes down. In comparison, the quantum capacitance is of the order of 4 pF/cm.[104] As a result, for CNTs, the quantum capacitance dominates over broad voltage ranges when operating in liquids. For graphene, the quantum capacitance varies linearly as a function of the applied gate voltage (due to the linear energy dispersion) and is around 25 μF/(cm^2.V).[76] At 10 mM ionic strength, the double layer capacitance is of the order of 5 μF/cm^2. As a result, both the double layer and the quantum capacitances affect the gate voltage characteristics especially at low gate voltages.

An important aspect in these configurations is that the contacts or metal leads that are used to contact the nanostructures are of the same size or larger than that of the nanostructure itself. Moreover, these contacts have been shown to dominate the electrical transport characteristics of both CNT and graphene devices.[105,106] In order to avoid contributions from contact resistance, a four-probe configuration may be utilized. However, ideally the contacts need to be isolated from coming in contact with the solution, in order to avoid any kind of interaction between the analytes and the immobilized receptors. It is clear that a failure to do so will alter the apparent active area of the sensing device.[16,97] In many sensor examples, receptors are immobilized everywhere on the device including the contacts. In such a situation the contacts also form part of the active surface and the advantages of high surface-to-volume ratio and the low surface – characteristics available only at a nanoscale – are not anymore guaranteed.[97] This may have consequences for the sensitivity and the detection limit of the realized sensors. In solutions this necessity to passivate the contacts is more stringent, in order to avoid any electrical shorts occurring through the background liquid. However, the stringency may be relaxed to a certain extent if the devices exhibit much lower resistivities than that of the surrounding solution. This is very often the case for metallic CNTs, CNT bundles/networks and graphene, when working in solutions of low ionic strength.[107,108]

Typical field-effect characteristics of devices fabricated using CNTs and graphene are collected in **Figure 8**. In most of the cases, the current at a fixed bias is measured as a function of the voltage applied to the gate electrode (reference electrode or back gate). When sweeping the gate voltage, the filling of the energy levels is continuously tuned, thereby moving from the conductance band (electron transport) into the band gap and subsequently to the valence band (hole transport). The variation in current is a few orders of magnitude for semiconducting CNTs and less than an order of magnitude for graphene and semi-metallic CNTs. Bundles and networks of CNTs predominantly show metallic or semi-metallic field-effect behavior. The measurement of current at a fixed voltage is simple, however, it is prone to noise and drifts especially in a liquid environment. A more elegant way is to measure the AC (alternating current) resistance or impedance (using a lock-in amplifier or

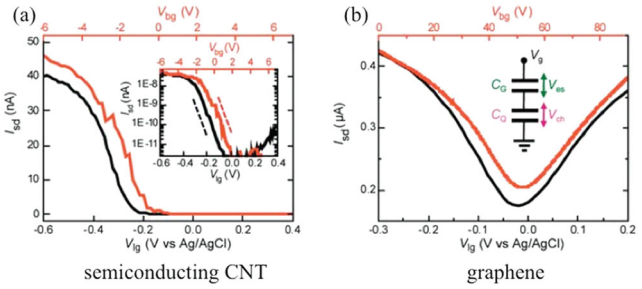

Figure 8. Field-effect characteristics of (a) a semiconducting CNT and (b) a graphene flake in the back-gated (black) and liquid-gated (red) configuration. Reproduced with permission.[103] Copyright 2009, Wiley-VCH.

an impedance analyzer) at a certain frequency as a function of gate voltage. This serves to reduce noise and minimizes drifts to a large extent. Using this strategy we have observed drifts of less than 10 mV over several hours with CNT-based liquid-gated field-effect devices.[109]

Instead of utilizing the resistance in a FET configuration as the sensor response, one could also measure the charge carrier density and mobility directly using a Hall bar or van der Paw configuration.[110] The advantage here is that the nature of the charge interaction occurring on the nanostructure surface can be unambiguously deciphered. This is, however, only feasible when using graphene-based sensors, since it is not possible to design Hall bars on CNTs. Using such a setup it was possible to detect charge transfer on to graphene from single NO_2 molecules in the gas phase as shown in **Figure 9**.[43] The type of charge transfer (as to electron donating or withdrawing) and the extent of charge transfer (the possibility to transfer individual electrons) could be deciphered through Hall bar measurements. Moreover, details of carrier density changes while varying pH and ionic strength or during DNA hybridization have been measured using a van der Paw configuration.[110,111]

Another possibility is to monitor changes in the charge distribution by electrochemical impedance spectroscopy (EIS).[112] Here, the impedance between an active electrode and the reference electrode is measured. In principle, the transistor configuration measures the same parameters using the nanostructure channel as an amplifier. The main difference in EIS is that a charge transfer mediator is additionally utilized, which increases the sensitivity of the sensor response. Although some reports exist, where standard EIS electrodes (such as glassy carbon) have been modified with graphene flakes, the actual role of graphene is not apparent in these measurements. In some cases, the impedance spectra of the solution have also been directly measured to detect the presence or absence of cells, for example with the help of vertically grown CNTs.[113] Direct detection of biomolecules is also possible using electrochemical methods.[114–117] However, we restrict our scope here mainly to FET-based transduction using nanoscale devices.

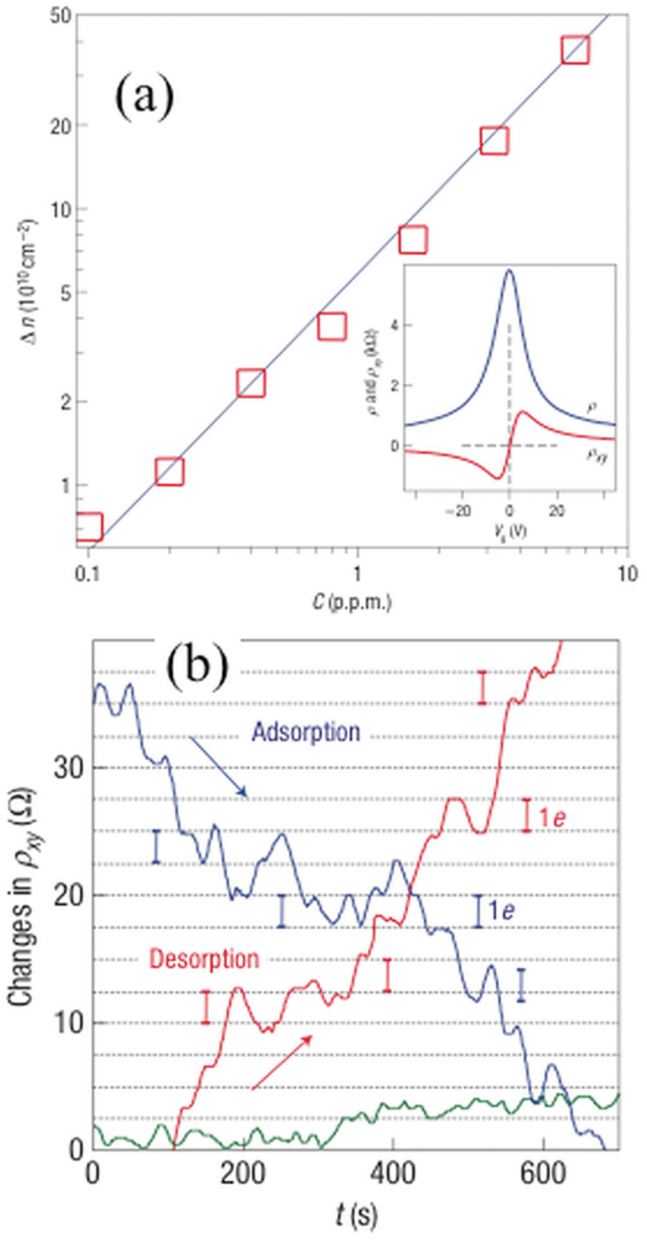

Figure 9. Influence of chemical doping on the electronic properties of graphene (a) Variations in charge carrier density as a function of the concentration of the dopant (here NO_2) measured using a Hall bar configuration. The inset shows raw measurement data plotting the transverse and longitudinal resistance from the Hall bar. (b) Discrete changes in Hall resistivity measured during the exposure of the sample to trace amounts of NO_2. The steps in the sensor response could be correlated with the transfer of electrons to and from graphene. Reproduced with permission.[43] Copyright 2007, NPG.

3.3. Selectivity: (Bio) Chemical Functionalization

Sensitivity and selectivity constitute fundamental performance parameters for any kind of biosensor. Due to their high surface-to-volume ratio, sensing devices based on CNS are inherently expected to exhibit high sensitivity. But this means also that they may respond to any kind of analyte in the environment. In order to be able to detect only a specific analyte or in other words to obtain selectivity, the surface of the nanostructure needs to be functionalized with an analyte-specific receptor. **Figure 10** gives an overview of different receptors that have been investigated on CNTs and graphene. As mentioned before, the receptor is a molecule that binds with a high degree of specificity to the analyte molecule sought for. In order to detect nucleic acids, the corresponding complementary base sequence is typically used. This is in most cases single-stranded DNA,[108,109,111] although other kinds of nucleic acids such as peptide nucleic acids (PNA) [118] have also been used as receptors. For the detection of proteins, antibodies can be utilized as receptors and vice versa.[119,120] Short nucleic acid sequences called aptamers have also shown good specifity for certain proteins, e.g., the thrombin aptamer for the protein thrombin.[121,122] Metabolites such as sugars constitute the next major category of biomoleucles.[123] Typically, enzymes involved in the chemical processing of the concerned metabolites are used as receptors.

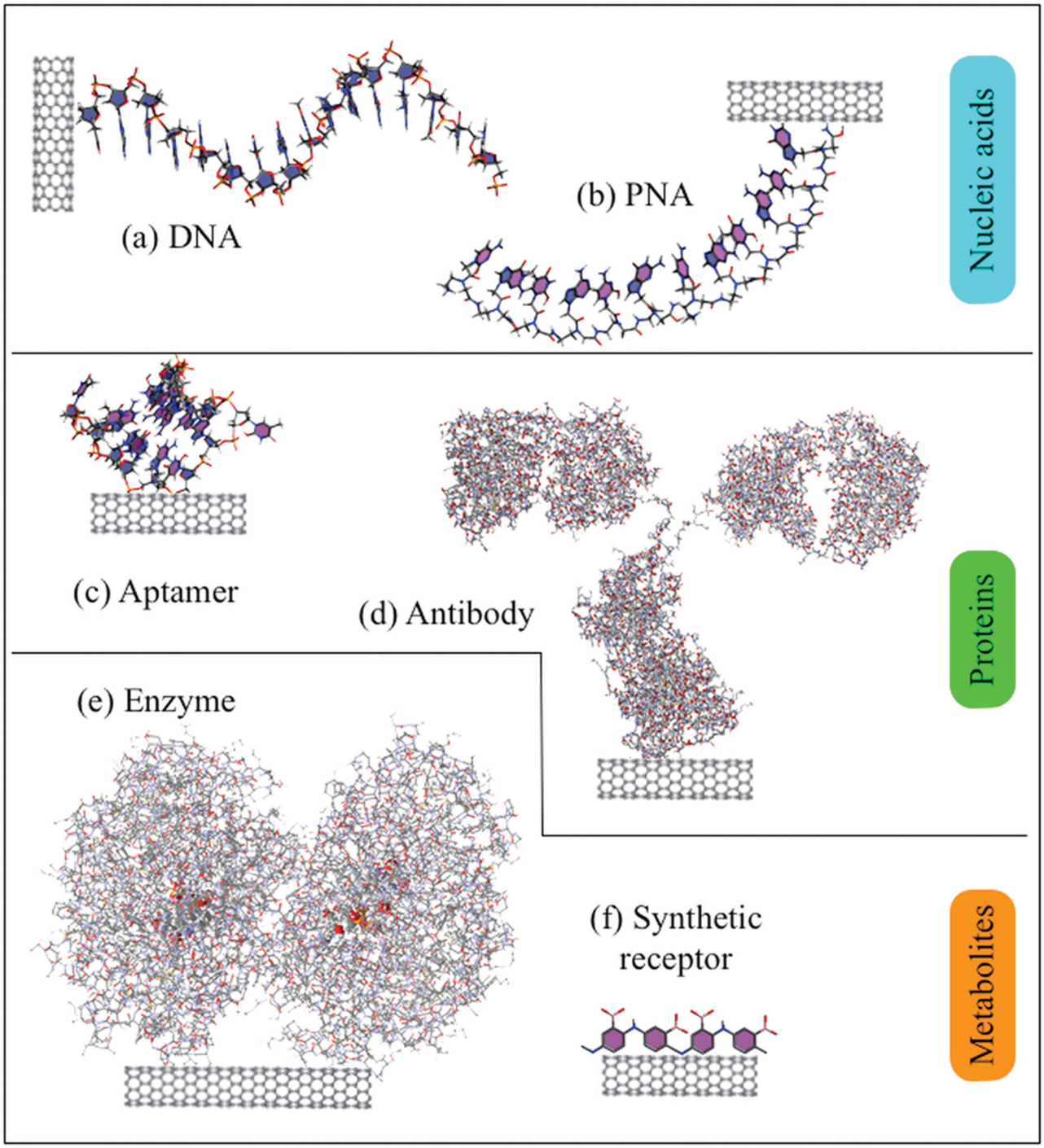

Figure 10. Attaining selectivity through an appropriate choice of receptors. A collection of typical receptors that are used for the realization of label-free detection of the three classes of analytes: nucleic acids, proteins and metabolites. (a) DNA: single stranded deoxyribonucleic acid (here: 16 bases) and (b) PNA: peptide nucleic acids (here: 12 bases) for the detection of DNA and RNA. (c) aptamers : short DNA sequences (here: thrombin aptamer) and (d) antibodies (here: an immunoglobulin antibody) for the sensing of peptides and proteins. (e) enzyme (here: glucose oxidase) and (f) synthetic polymers (here: poly(3-aminophenylboronic acid)) for the detection of metabolites such as sugars.

Alternatively, synthetic polymers for the detection of sugars can also be deployed as receptors.[124] It is apparent that the biochemistry of the concerned analyte dictates the choice of the receptor and thereby the selectivity of the sensor. The challenge is to implement this chemistry on the nanostructure surface in an efficient manner.

Various chemical functionalization protocols have been reported to attach receptors on to the surface of CNTs and

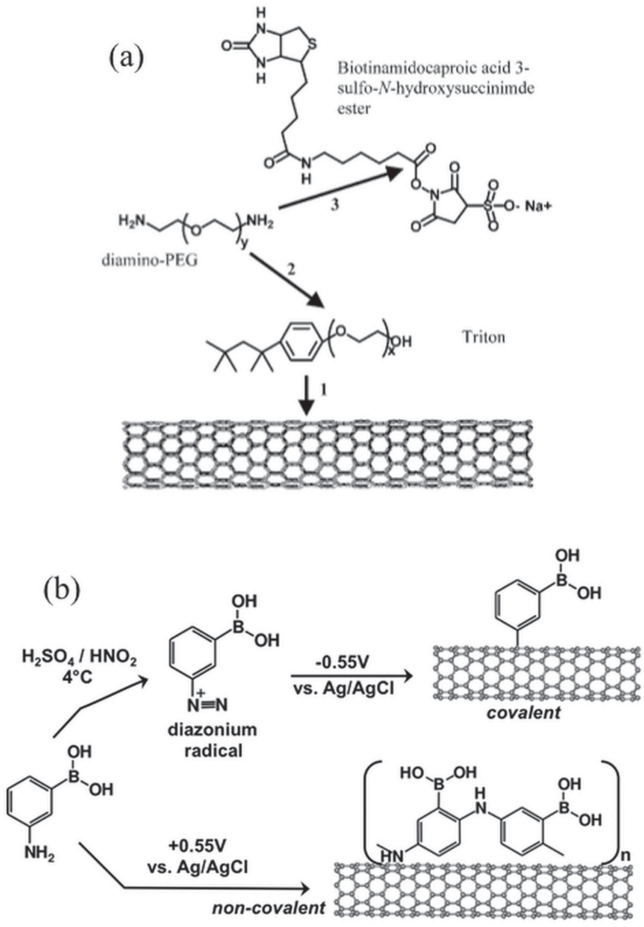

Figure 11. Typical examples of functionalization protocols used for the attachment of receptors on to carbon nanotubes. (a) Incubation-based strategy. Here hydrophobic interactions between a surfactant (Triton) and the CNT are utilized to attach a conjugated biotin non-covalently on to the surface of CNTs. (b) Electrochemical modification showing one possibility to obtain the same functional moieties (boronic acid) either in a covalent or non-covalent manner starting from the precursor 3-aminophenyl boronic acid. *(a)* Reproduced with permission.[125] Copyright 2002, ACS.

graphene. These methods can in general be classified under two categories, namely simple incubation and electrochemical modification (see **Figure 11**). Incubation-based methods involve the exposure of the graphene or nanotube surface to a solution containing the receptor molecules. This may be done by spotting or spin coating the receptor solution on the device surface. In order to obtain maximal sensitivity and exploit the inherent advantages of nanostructures, it is beneficial to realize the functionalization exclusively on the nanostructure surface. For this purpose, some kind of chemical coupling between the receptor and CNS surface needs to be incorporated. Nonetheless, in many cases sensors have been demonstrated without this chemical coupling. In this situation the whole surface is covered with receptors. Although a sensor response is discernible in such devices, it can be expected that by a controlled attachment of the receptors on to the CNS surface, the sensitivity and detection limit can be further improved.[16,97]

The chemical coupling between the receptor and the CNS may be non-covalent or covalent. For the former case, hydrophobic interactions (see Figure 11(a)) or pi-pi interactions between aromatic linkers and the sp^2-bonded carbon network or polymer coatings[33,125] have been successfully utilized to attach a high density of receptors. In the case of oxidized nanotubes or chemically derived graphene – with a high density of oxygen containing groups – the receptors can be directly covalently coupled using heterobifunctional linkers.[53,55,56] For this purpose, the carboxyl or epoxide groups are activated in a first step followed by conjugation of the receptor with the help of an amino group. Many of the receptors to be attached already contain amino groups (e.g., antibodies). In other cases, they may be modified with amino groups (e.g., amino functionalized oligonucleotides) prior to the attachment.[109,126,127] This is a very efficient strategy to covalently attach the receptors on to the oxidized CNS surface.

Electrochemical functionalization represents a more versatile strategy to attach receptors on to the surface of CNSs.[80,128] It involves the creation of a reactive species from a precursor in solution, by passing a current (galvanostatic) or applying a voltage (potentiostatic). Under these conditions, a reactive species is formed through charge transfer to or from the CNS. This reactive species subsequently attaches itself to the CNS surface. Many of the reactive species have a tendency to react with the precursor leading to self-polymerization resulting in polymeric layers on the CNS surface.[129] Through a smart choice of the precursor and appropriate control over electrochemical conditions, it is possible to control the density of attached receptors.[130,131] Moreover, the nature of the coupling (as to being covalent or non-covalent) can be tailored by choosing an appropriate reactive functional group of the precursor.[129] The ability to controllably attach receptors in a covalent manner on the CNT surface has enabled the use of even metallic CNTs as active elements of pH sensors.[107] By varying the nature of coupling and keeping the receptor functionality constant (in this case a boronic acid receptor for the detection of sugars, see Figure 11(b)), we have demonstrated that the covalent or non-covalent nature of the coupling has a significant influence on the sensing mechansims, as discussed below. Electrochemical functionalization of graphene has also been reported, though it has rarely been used to obtain label-free sensing devices.[80,132] Most of the biological receptors have hydrophobic compartments and the incubation-based strategy seems to work good enough to obtain a fairly well functionalized graphene surface.

When using intermediate linkers, it is important that the thickness of these layers must be kept as low as possible. This is due to the fact that field-effect sensors are maximally sensitive to charge variations mainly within the electrical double layer.[133] As a result, it is necessary to have the binding event occurring very close to the nanostructure surface or at the interface with the liquid. However, other mechanisms have also been proposed which are not completely restricted to processes occurring inside the double layer. One possibility is the rearrangement of the counterion layer after the binding event takes place.[101]

In the above discussion we have restricted ourselves to those functionalization methods that have been successfully utilized for the demonstration of biosensors. Needless to say, there are

a number of other general methods to obtain a range of functional groups on the CNS surface. We refer the readers to other focused reviews on this topic.[17,74,134–139]

3.4. Sensing Mechanisms

In order to obtain viable sensors and subsequently use them for realistic applications, it is essential to understand the mechanisms behind the sensor response. These have been widely investigated for the case of nanotube sensors and further information is available from data on nanowire sensors. Most of these mechanisms also apply for the case of biodetection using graphene. There are basically four mechanisms that have been theoretically proposed to account for the sensor response: (i) contact effects, (ii) charge transfer or doping, (iii) screening or capacitance variations and (iv) charge scattering or mobility changes.[35,140] We will first discuss the case of the effect of Schottky barrier formed at the nanostructure-metal contact. When semiconducting CNTs are contacted by metals a Schottky barrier is formed.[106] Similarly, contacts have also been shown to dominate transport in metallic CNT and graphene devices.[105,141] If receptors are present at the contacts, the binding of the analyte molecules to these receptors can modulate the Schottky barrier characteristics. Binding events happening at these potential barriers may hence dominate the sensor response.[119] In order to minimize this contribution, the electrodes need to be passivated. This is especially beneficial when performing sensor trials directly in liquids.

Once the contribution from the contacts is eliminated, the variation in charge distribution occurring at the CNS surface can be mainly observed as a charge transfer doping effect in the field-effect characteristics (**Figure 12**(a)). Typically, the sensor response is shifted to the left or right on the gate voltage scale, with minimal changes in the other aspects of the field-effect behavior. The exact mechanism of how this charge variation brings in the shift in gate voltage characteristics may be two-fold: either by just acting as an additional gate on the CNS surface or by a realistic charge transfer on to the underlying CNS. It is difficult to distinguish the two from the FET characteristics alone; Hall bar and/or capacitance measurements may help in identifying the real mechanism behind the shift. In case the binding is reversible, the original situation can be recovered. This is the dominant mechanism, when the receptors are non-covalently attached to the CNS surface.[119,124,140]

Variations in the charge environment on the surface may also lead to a change in the interfacial capacitance. This results in a change in the efficiency of gating characteristics, which in turn modulates the slope of the sensor response as shown in Figure 12(b). This can be understood by visualizing that the binding of the analyte on to the CNS surface leads to a change in the dielectric constant of the electrical double layer thereby affecting the slope of the gate voltage characteristics. In the case of CNTs, this change in capacitance can only be detected weakly as the quantum capacitance dominates the FET behavior.[73] By contrast, it may be expected that with graphene devices, this effect is comparatively stronger. However, due to the low ON-OFF ratio of graphene FET characteristics, this mechanism has not yet been shown to have a considerable effect on the sensor response.[110]

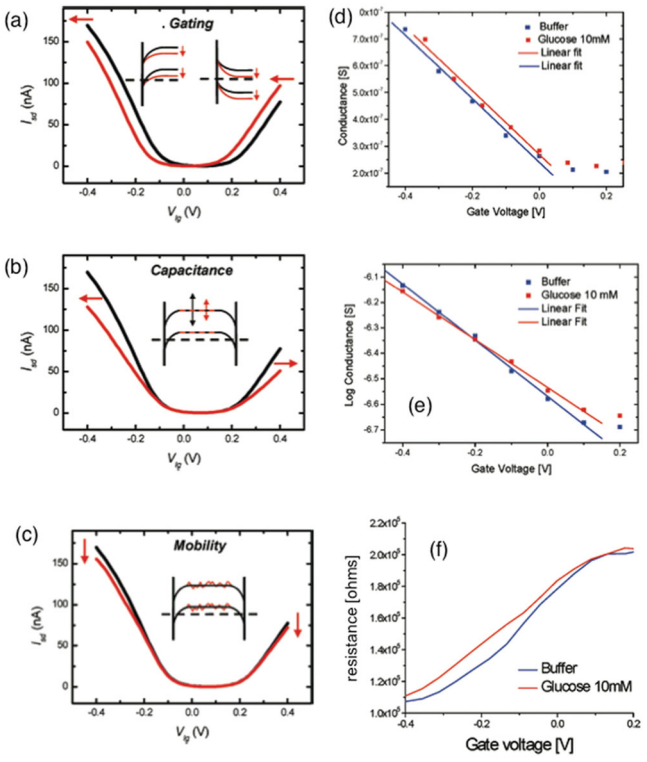

Figure 12. Sensor mechanism of CNT-FET-sensors. *Theory*: Predicted sensor response based on various sensing mechanisms: (a) Surface Charge/Gating (b) Screening/Capacitance and (c) Charge scattering/Mobility. *Experiment*: Sensor response to glucose of (d,e) non-covalently and (f) covalently functionalized CNT sensors. In (a) the occurrence of or a change in the surface charge leads to a shift in the gate voltage characteristics, while in (b) a change in capacitance is observed due to screening of the gate potential by the anlaytes bound onto the CNT surface. These two cases are observed in experiments where the SWCNTs are non-covalently functionalized with the phenylboronic acid moieties. A shift in the threshold voltage (d) and a change in the slope (e) is observed in the experiments. In (c) the binding of analytes on to the sensor surface leads to changes in the strength of charge scattering resulting in an increase of resistance at all gate voltages. Experimentally this condition is observed for the SWCNT devices covalently functionalized with phenyl boronic acid moieties (f). Reproduced with permission.[140] Copyright 2008, ACS and[124] Copyright 2010, ACS.

The fourth mechanism involves direct interaction between the binding event and the electronic structure of the CNS. This could for example be a modulation of the mobility or a variation in the scattering cross-section for electronic transport.[107,121,124] As a result, the field-effect characteristics show a suppression of conductance for the entire gate voltage range as shown in Figure 12(c). In order to achieve this, it is necessary to covalently attach the receptor on to the CNT surface. Based on this mechanism, we have demonstrated a pH sensor by covalently attaching diethylaniline moeities on to individual metallic CNTs.[107] The attached receptors function as analyte-specific charge scattering centers, whose scattering strength is modulated by the pH of the solution. The occurrence of the latter three mechanisms has also been consistently observed

in contact-passivated CNT-based sensors.[35] For this purpose we have realized sensing devices for sugars by attaching boronic acid moieties either covalently or non-covalently. In the former case, the scattering mechanism dominates the sensor response, while in the non-covalently coupled devices, both doping and capacitance variations could be observed (see Figure 12(d–f)).

4. Performance Merits of Biodetection Using Carbon Nanostructures

In this section, we collect reported results on the sensitive detection of biomolecules using CNTs and graphene. First, we present sensors demonstrated for the detection of nucleic acids followed by proteins. In both cases, extremely low detection limits have been observed, making such nanoscale sensors competitive with current classical assays. Subsequently, we review progress towards observation of single enzyme activity using CNT-based devices. Finally, we discuss issues that are crucial in determining the sensitivity of the nanoscale biosensors.

4.1. Pushing the Limits of Label-Free Nucleic Acid Detection

Nucleic acids constitute an important class of analytes, whose detection is vital, both for fundamental research as well as for diagnostic purposes.[142,143] Detection of DNA using CNT-based sensors has been demonstrated as early as in 2006.[108,144] A complementary DNA sequence is used as the receptor, however, other candidates such as Peptide Nucleic Acids (PNA) have also been evaluated as receptors.[126] At the initial stages, back-gated field-effect characteristics were predominantly used as sensor response, as shown in **Figure 13**(a).[108,144–146] Furthermore, in most of the cases the incubation strategy was used to obtain the receptors on the entire sensor surface. Moreover, the electrodes were not passivated and hence the possibility of binding events occurring on the contact areas could not be completely excluded. The lowest detection limit using such type of sensors is in the picomolar range.[108] The detection limit can be improved to the high femtomolar range, when the hybridization is augmented with additional steps such as use of a secondary probe and nanoparticle labeling.[147] **Table 1** presents a collection of sensors reported for the direct label-free detection of nucleic acids using CNT- or graphene-based devices.[148] It is apparent that CNT devices fabricated with contact passivation where measurements are performed directly in liquids exhibit the lowest detection limits.

Using the controlled electrochemical functionalization strategy coupled to a sensitive detection scheme (combining impedance spectroscopy and FET measurements) we have obtained a detection limit as low as 100 aM using CNT-bundle transistors, as shown in Figure 13(b).[109] This is the lowest detection limit ever reported for the direct one-step label-free indicator-free detection of nucleic acids without the use of complex reaction schemes or sandwich protocols.[148] Hence, this assay raises hope for its use in the detection of ultralow amounts of nucleic acids probably even avoiding PCR. A first step in this direction has already been demonstrated by evaluating the sensor response in a heterogeneous mixture of many nucleic acid sequences where the target constituted only 2% of the test solution. A detection limit of 200 aM could be achieved here.[109] Another example is the observation of femtomolar limit for the detection of RNA using liquid-gated CNT devices functionalized with PNA.[126]

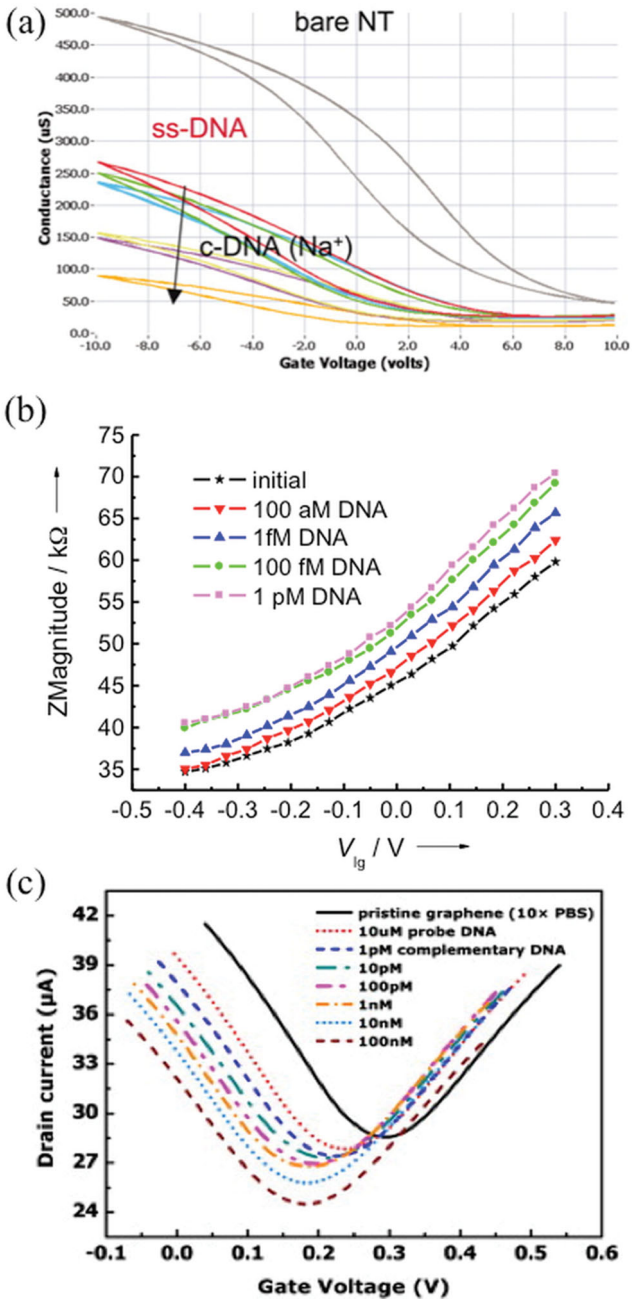

Figure 13. Comparison of sensor responses for the detection of DNA using (a) CNT network sensors – back-gated configuration, dry state (b) CNT bundle sensors – liquid-gated configuration, in buffer (c) CVD-graphene sensors – liquid-gated configuration, in buffer. (PBS – Phosphate buffer saline). Reproduced with permission.[108] Copyright 2006, National Academy of Sciences USA;[109] Copyright 2011, Wiley-VCH and[149] Copyright 2013, Elsevier.

Table 1. Label-free carbon nanostructure field-effect biosensors for the direct detection of DNA and RNA.

Biosensor architecture	Detection mode	Passiv-ation[a]	Probe attachment	Analyte	Imm.Time/ Response time	Detection limit	Concentration Range	REF
Pt – SWCNT bundles – Pt	In buffer (liquid gate)	Yes	EDC/NHS coupling with amino DNA (electrochemical)	24 bp synthetic DNA	1 h/30 m	100 aM	100 aM – 1 pM	[109]
Au – SWCNT – Au	In buffer (liquid gate)	Yes	Incubation[b] in amino terminated PNA	12 bp synthetic RNA	NR/few min.	500 fM	500 fM, – 5nM	[126]
Ti – SWCNT network – Ti	Dry (back gate)	No	Incubation[2] in unmodified DNA	12 bp & 51 bp synthetic DNA	1 h/1 h	1 pM	1 pM – 100 nM	[108]
Ti – SWCNT – Ti	In buffer (liquid gate)	No	EDC/NHS coupling with amino DNA (electrochemical)	10 bp synthetic DNA	14 h	100 nM[3]	100 nM – 1 mM[c)]	[127]
Au – SWCNT network – Au	In buffer	No	Incubation[2] in thio-lated DNA	15 bp & 30 bp synthetic DNA	22 h/20 m.	100 nM	NI	[132]
Au – SWCNT network – Au	Dry (back gate)	No	Incubation[2] in amino-terminated DNA	12 bp synthetic DNA	16 h/1 h	500 nM	NI	[145]
Co – SWCNT – Co	Dry (no gate)	No	EDC/NHS coupling with amino DNA (to COOH groups of CNT)	20 bp synthetic DNA	12 h/12 h	500 nM	NI	[146]
Pd – SWCNT – Pd	Dry (back gate)	No	EDC/NHS coupling with amino DNA (to synthetic polymer on CNT)	20 bp synthetic DNA	8 h/2 h	16.2 mM	NI	[33]
Ag – CVD-G – Ag	In buffer (liquid gate)	Yes	Incubation with thio-lated probe DNA	12 bp synthetic DNA	16 h/4 h	1 pM	1 pM – 100 nM	[149]

[a)]If electrodes are passivated, the nanotubes exclusively constitute the active area. Otherwise, the electrodes are also decorated with probe nucleic acids; [b)]Incubation implies that the sample was left in a solution of probe DNA for a long time usually several hours. The probe DNA is not chemically coupled to the CNT surface; [c)]In this work the kinetics of DNA hybridization were investigated with single-molecule resolution.

By contrast, the best detection limit for nucleic acids using graphene devices has been in the high picomolar range[149,150] as is apparent from Table 1. Such a high detection limit may be partly attributed[151] to the active surface of CVD-graphene used here, which is more than 3 orders of magnitude larger than that of CNTs (see Figure 13(c)). However, graphene devices have contributed more to the understanding of mechanistic aspects of DNA hybridization on the nanostructure surface. For example, using Hall effect measurements in a van der Paw configuration the underlying mechanism of the sensor response in a large area graphene device (cm scale) was investigated.[111] It was inferred that the carrier concentration increases, while mobility decreases upon hybridization of the target DNA with the immobilized probe. This is consistent with a shift in the gate voltage characteristics towards negative gate voltages for both graphene and CNT-based liquid-gated devices.[109,150] Furthermore, it was observed that effective hole density changes as a function of DNA concentration.

Subtle differences in the sensor response could be observed when the graphene device was exposed to oligonucleotide sequences with a single base mismatch.[150] Similar behavior has also been observed earlier using CNT-based devices.[108,127] However, the sensitivity when using the van der Paw configuration was slightly better. DNA sensors are also ideally suited to investigate the effect of ionic strength on the sensor response. Using the two-probe FET measurement setup it could be shown that the sensitivity or the slope of the sensor response varies as a function of the ionic strength of the solution, as shown in

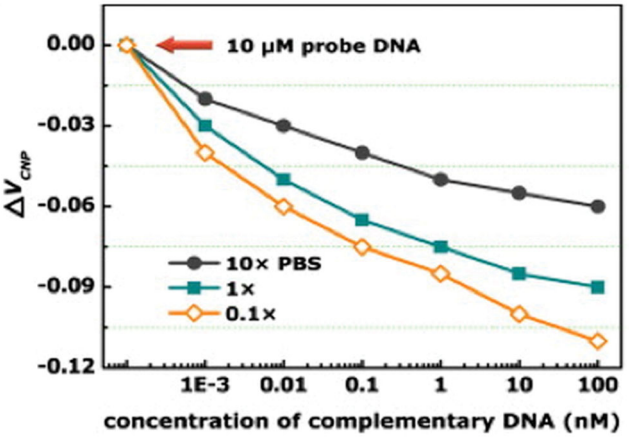

Figure 14. Effect of the ionic strength of the solution on the liquid-gated sensor response of CVD-graphene sensors for the detection of DNA. It is apparent that with increasing ionic strength (from 0.1X to 10X), the sensitivity of the sensor deteriorates. (PBS – Phosphate buffer saline). Reproduced with permission.[149] Copyright 2013, Elsevier.

Figure 14.[149] A lower sensitivity was observed at higher ionic strengths, which was attributed to minimized charge impurity scattering caused by the DNA molecules[152] and differences in the thickness of the electrical double layer.[57]

4.2. Detection of Proteins and Microorganisms

While the detection of short sequences of nucleic acids in trace amounts is mainly suited for specialized purposes, the detection of proteins at ultralow concentrations is interesting for a wide range of applications. Unlike the case of nucleic acids, the goal here is to be sensitive enough in the relevant concentration range that is meaningful for a specific diagnosotic purpose. On the other hand, the ability to detect concentrations lower than this range is expected to open new avenues for therapy and diagnostics.[13] Proteins are in general more "sticky" than nucleic acids and specialized passivation techniques are necessary to ensure that they do not adhere to electrode surfaces and substrates.[119,153] This can be avoided to some extent using (poly) ethylene glycol-based linkers, which provide resistance towards biofouling of the sensor surface.[154] As a prototype for the detection of proteins, the biotin – sptreptavidin system is often utilized.[155] Many CNT-based sensors have been demonstrated with varying limits of detection for a range of proteins such as the cancer biomarker PSA (prostate-specific antigen),[156] antibodies such as immunoglobulin E[157] and common proteins such as bovine serum albumin (BSA)[153] and thrombin (see **Figure 15**(a–d)).[158] In general, the corresponding antigen or antibody functionalized on to the CNT surface functions as the receptor. Also, specialized nucleic acids called aptamers[159] have been successfully deployed as receptors for the detection of BSA and thrombin. Typical detection limits for proteins using CNT devices are in the picomolar or in the low ng/ml range. This is very close to the pg/ml limits attainable using the gold standard for immunoassays namely ELISA (Enzyme-linked immunosrbent assays).[160] It is worth mentioning that in many of these cases the contact electrodes were not passivated and the Schottky barrier mechanism was found to play a dominant role in the sensing process.[119] Liu et al. have demonstrated a completely different strategy by introducing the receptor molecules covalently into individual nanotubes.[121] Here, gaps are introduced in oxidized CNTs which are bridged by coupling to amino functionalized receptors. The binding of analytes on to these receptors leads to prominent changes in the electrical properties.[161] By introducing a thrombin aptamer, they could demonstrate the detection of thrombin in the attomolar range, which is better than the detection limits attainable by ELISA.[121]

Very few reports have so far addressed the possibility to detect proteins using graphene devices.[57] Using exfoliated graphene and aptamers as receptors immunoglobulin E could be detected down to the low nanomolar (μg/ml) range in a liquid-gated configuration.[162] In order to ensure that the binding of the proteins occurs within the electrical double layer, just the antigen-binding part of an antibody (Fab fragment) has also been evaluated as candidate receptors.[120] Using this construct, heat shock proteins could be detected down to the low nanomolar range. In both these cases, the receptor is non-covalently coupled to the graphene surface and the binding of the proteins lead to a shift in the gate voltage characteristics (see Figure 15(e,f)). Other reports are based on the use of chemically derived graphene devices. With the help of nanoparticle-conjugated antibodies as receptors, immunoglobulin G (IgG) could be detected in the μg/ml range.[163] Here, the nanoparticle conjugates were just immobilized by van der Waals forces and the measurements were made in the dry state. We have exploited the presence of oxygen functionalities on the RGO surface to attach antibodies for the detection of amyloid beta (Aβ) peptides (see Figure 15(g,h)),[53] which have an important implication in Alzheimer's diseases.[164] In contrast to other immunoassays, the receptors here are bound covalently to the underlying graphene structure. This enables a detection limit in the low pg/ml range, which is an order of magnitude lower than what is currently achievable using ELISA for Aβ detection in biological fluids.[165] Due to the covalent modification, the sensor response could be correlated to the scattering mechanism described earlier. Although, carbon-based sensors appear competitive against standard immunodetection methods such as ELISA, SiNW-based sensors exhibit comparatively lower detection limits and higher sensitivity.[15] For example, SiNW-based sensors have been shown to detect streptavidin (with biotin as the receptor) down to concentrations as low as 10 fM, an order of magnitude lower than those attainable using CNT-based sensors.[166,167] Moreover, detection of cancer markers such as PSA or Carcinoembryonic antigen (CEA) has been possible down to the pg/mL range.[168] The reason for the higher sensitivity may be partly attributed to the different doping levels in silicon nanowires in comparison to that of carbon-based devices and the actual protocol utilized for surface functionalization.[169]

Besides proteins and small peptides, direct detection of bacteria has also been reported.[7,54] Naturally, for the detection of such microorganisms, graphene-based devices are more suited since the sizes of the graphene flakes are typically of the order of the size of a single bacterium.[170,171] By contrast, an individual nanotube is around three orders of magnitude smaller than that of a single bacterium. Nonetheless, networks of nanotubes have been utilized to detect pathogenic microorganisms such as *Escherichia coli*, *Salmonella infantis* and *Bacillus cereus* (see **Figure 16**).[54,172,173] Analogous to the case of proteins, the receptors comprise of antibodies specific to the microorganism or aptamers that are known to bind to a membrane protein of the bacterial cell. In general, the binding of the microorganisms to these receptors leads to drastic changes in the electrical response, whose exact mechanisms remain to be explored. A major drawback in all these experiments is that there has been limited proof for the selectivity of the sensor response towards the microorganism of interest. This is critical since the microorganisms tend to stick non-specifically on to surfaces, especially on to hydrophobic surfaces such as graphene or nanotubes. Such non-specific binding (NSB) has to be effectively suppressed when deploying such sensors for a specific application. In addition to the direct detection of the presence of bacterial cells, the action potentials related to the activity of electrogenic cells could be monitored in real time.[170] The use of graphene for this purpose presents a key advantage due to the favorable low

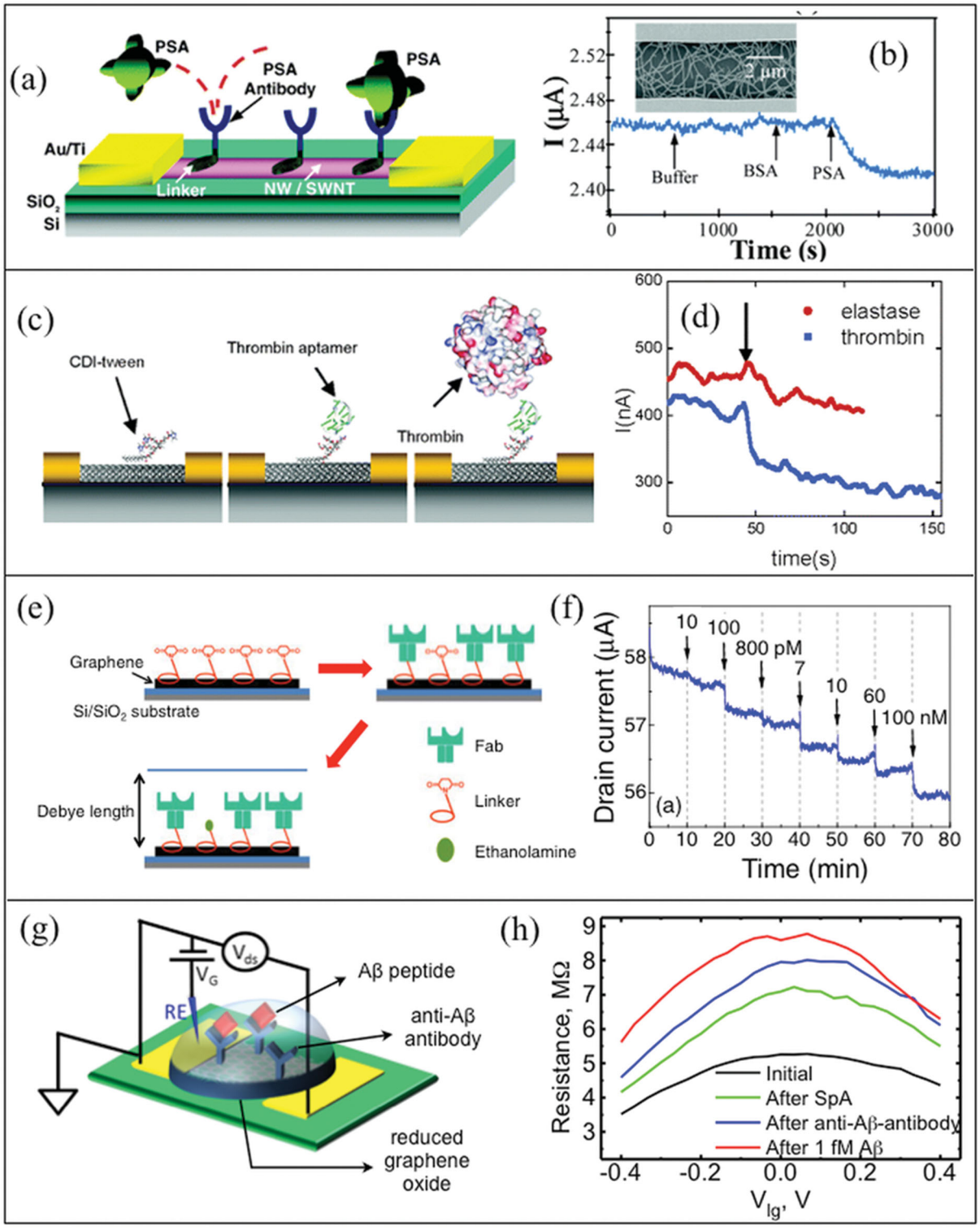

Figure 15. Comparison of sensor responses for the detection of proteins using CNT and graphene sensors. (a) Schematic and (b) sensor response of a CNT network sensor for the detection of the cancer biomarker PSA (prostate specific antigen). (c), (d) Detection of thrombin using an aptamer immobilized on the nanotube surface – Schematic of the detection protocol (c) and sensor response (d) showing sensitivity towards thrombin. (e), (f) Detection of heat shock proteins (HSP) through the use of an antibody fragment (Fab) as the receptor. Schematic of the receptor functionalization protocol (e) and sensor response to increasing concentrations of HSP (f). Detection of amyloid beta peptides using the corresponding antibody on a reduced graphene oxide sensor – Schematic (g) and sensor response (h). SpA refers to protein A that is used in the first step to limit non-specific binding. Reproduced with permission.[156] Copyright 2005, ACS;[158] Copyright 2005, ACS;[120] Copyright 2012, Japanese Society of Applied Physics and[53] Copyright 2012, ACS.

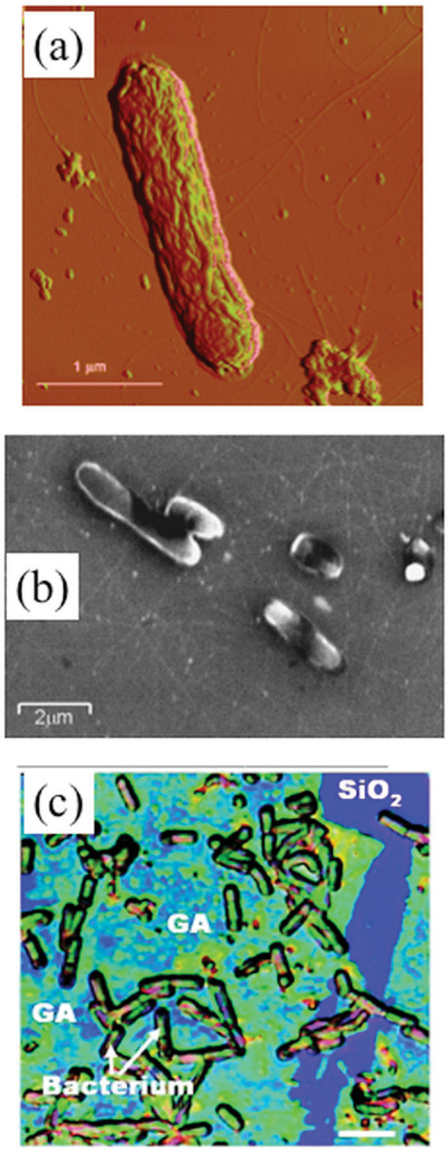

Figure 16. Images showing the deposition of bacteria on various CNS-based sensors. (a) AFM image of *Escherichia coli* bound to aptamer functionalized CNT-network sensors. (b) SEM image of *Salmonella infantis* attached to antibody functionalized carbon nanotube network sensors. (c) Optical image showing the attachment of bacterial cells (*Bacillus cereus*) onto chemically derived graphene sensors (GA – amino functionalized reduced graphene oxide). Reproduced with permission.[172] Copyright 2008, Wiley-VCH;[173] Copyright 2008, Elsevier and[54] Copyright 2008, ACS.

noise characteristics and the high trannsconductance readily available in such devices.

4.3. Towards Observing the Activity of Single Enzymes

The ability to realize highly sensitive biomolecular detectors using CNTs motivates the development of protocols that might allow for the observation of the activity of single enzymes. Towards this purpose, point defects have been introduced in

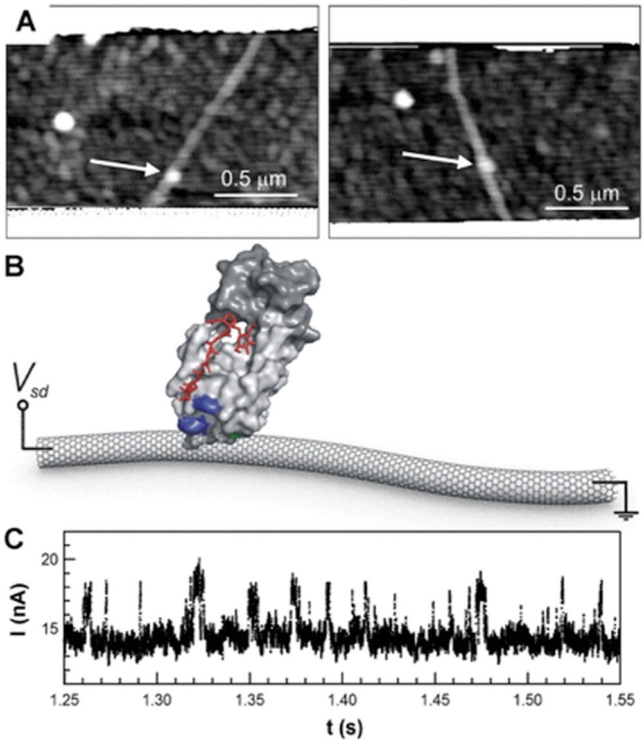

Figure 17. Detection of single-molecule enzyme activity using individual CNT devices. (A) AFM images of CNT devices functionalized with a single molecule of the enzyme lysozyme. (B) Schematic of the device showing the protein molecule attached to the CNT and the measurement configuration. (C) Typcial sensor responses observed on such devices, where the spikes are corroborated to turnover events where the enzyme processes its substrate peptidoglycan. Reproduced with permission.[175] Copyright 2013, ACS.

CNTs and subsequently functionalized with individual enzyme (lysozyme) molecules (**Figure 17**(a,b)).[174,175] The activity of the enzyme molecules could be monitored upon introduction of the enzyme substrate (peptidoglycans) in real-time. To this end, the liquid gate was kept at a constant potential and the current continuously monitored at a very high rate as a function of time. By performing a statistical analysis of the shot-noise-like signals (Figure 17(c)) observed in such experiments, it was concluded that it is possible to observe the individual turnover events during the enzyme activity.[176] The turnover rates measured using this method were consistent with those obtained from fluorescence correlation spectroscopy (FCS). It was proposed that mechanical distortions and dynamic motion occurring during the turnover leads to the pulses in the current signals. However, the magnitude of these pulses increased monotonously with decreasing ionic strength and did not completely correlate with the enzymatic activity observed in the optical measurements. The underlying mechanism behind these responses is not completely clear, although using eight different lysozyme variants it was found that the charge on the protein molecule is responsible for the sensor responses.[175] Specifically, in these variants, different amino acids were substituted at two specific locations in the protein molecule. The sign of the current change could be correlated with the charge on the amino acid that was introduced in the corresponding

variant. It is expected that new information related to the behavior of enzymes may be gathered using this technique, analogous to work on FCS[177,178] and electrochemical correlation spectroscopy,[179] with the advantage that it is label-free.[180] Nevertheless, it is worth considering that such a detection method is interesting mainly for fundamental studies, and is not amenable to high sensitivity diagnostics due to the high bulk concentration of analyte molecules involved here.[13]

4.4. Sensitivity Issues

From the foregoing discussions, it is evident that there are a number of advantages when deploying CNS devices in a FET configuration for the detection of biomolecules. However, one of the major concerns is the spatial extent from the nanostructure surface within which the binding event can be efficiently sensed by the underlying nanostructure. This range is believed to be restricted to the thickness of the electrical double layer.[57,181] At typical ionic strengths of around 100 mM, this layer is less than a nanometer in thickness.[16] The sensor response itself may be strongly limited by the screening introduced by the high density of ions present here.[110,150] As a consequence, the sensitivity to the binding event is restricted to a small region in the vicinity of the nanostructure. Due to these reasons, it is necessary to have the receptor immobilized directly at the solid-liquid interface. By contrast, in other label-free sensing techniques such as surface plasmon resonance (SPR), this sensitivity zone is of the order of 50 to 100 nm.[182] One workaround that is often proposed to improve the sensitivity is to perform the detection at a lower ionic strength. However, it has been argued that this may introduce additional complexities to the detection protocol and / or affect the nature of the biomolecular interaction itself.[57] Very few controlled and systematic experimental studies are available to confirm these hypotheses.[150]

One way to to tune the sensitivity is to utilize covalent functionalization of the receptor on to the CNT surface.[128] In this method, the receptor disrupts the correlated electron transport on the nanostructure surface.[129,183] We have demonstrated that it is indeed possible to gain control over sensitivity by varying the density of functional groups on the sensor surface.[131] Through every subsequent electrochemical attachment of diethylaniline moieties to metallic CNTs in a covalent manner, the sensitivity towards pH could be gradually increased (see **Figure 18**).[35] In principle, through the use of covalent attachment it has been possible to observe the activity of individual enzyme molecules,[176] as well as to attain a sensitive detection of proteins down to the attomolar level.[121] However, there is a tradeoff when using covalent functionalization, namely that the underlying sp^2-bonded network suffers disorder with every round of covalent functionalization and the sensitivity cannot be increased infinitely without loss of the favorable electrical characteristics of CNTs.

5. Future Prospects

The fundamental mechanism by which carbon nanostructure-based devices sense biomolecules is through the detection of charge or changes in charge distribution on their nanoscale surface. Since carbon nanostructures are extremely sensitive

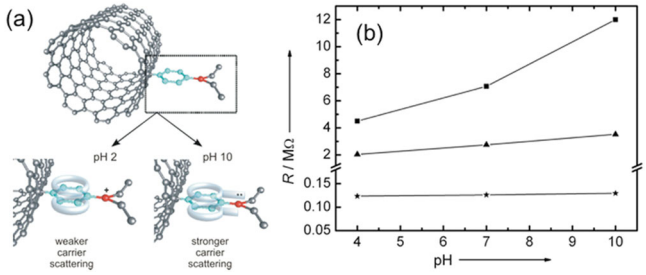

Figure 18. Controlling the sensitivity of CNT devices through covalent electrochemical modification. (a) Schematic of the detection protocol for a pH sensor, using covalently attached diethylaniline moieties as receptors. The bottom two images depict the variation in the surface charge distribution at two differnt pH. (b) Sensor response before (circles) and after first (triangles) and second (squares) covalent electrochemical modification of a metallic CNT device with diethylaniline moieties. Reproduced with permission.[107] Copyright 2007, Wiley-VCH.

to their environment, much of the research is directed towards demonstrating absolute sensitivity or single molecule detection.[7,184] In a number of experiments the capability to detect the interaction of individual molecules on the CNT or graphene surface has been reported.[43,175,176] However, strictly speaking such devices are able to resolve the interaction of individual species on the nanostructure surface rather than detect them.[185] In such single molecule resolution experiments, the bulk concentration of the analyte is typically much higher (in the nanomolar range for e.g.), and individual binding events are followed in real time. While such experiments are well suited for evaluating the mechanisms of biomolecular interactions, it is rather difficult to deploy these methods in the context of practical sensing applications, where the aim is to reduce detection limits to ideally as low as a single molecule in the test solution. Nevertheless, these methods highlight the feasibility to detect as low as a single unit of charge.

The real limits of single molecule detection are rather set by limitations arising due to measurements made directly in liquids. Although the possibility to detect a single unit of charge has been demonstrated in the gas phase, a major hurdle in liquids is the presence of ions, which tend to screen the interactions occurring at the nanostructure/biomolecule interface. Theoretical aspects of these interactions have been the focus of a number of studies.[101,186,187] First, the balance between the quantum capacitance (C_{qm}) of the underlying nanostructure and the capacitance of the electrical double layer (C_{edl}) has a considerable effect on the sensitivity of the detector (see Figure 7).[73,75,188] At high ionic strength the thickness of the double layer is less than a nm, and it has been calculated that the charge sensitivity is minimal in this case in comparison to operation at low ionic strengths.[133,181,187] However, at low ionic strength, biomolecular interactions may not be optimal. Moreover, it has been theoretically estimated that at low analyte concentrations the diffusion of analyte species towards the nanoscale surface is restricted thereby requiring long incubation times for the detection of trace amounts of molecular species.[185–187,189] This has important consequences for the observed binding kinetics. In spite of these theoretical speculations, a number of experiments have demonstrated high

sensitivity within practical timescales. This is most likely due to the fact that it has been difficult to incorporate all aspects of an experiment in theoretical simulations. One example includes electrostatic or electrodynamic effects that are usually neglected in simulations – which are obviously present in field-effect sensors.[190] Such effects are expected to have a major influence on the diffusion of species towards the sensor surface as well as the binding process. Along these lines, one of the fundamental challenges for the future is to investigate the kinetics of binding at the nanoscale in a more elaborate manner in order to arrive at realistic detection limits and identify if it would indeed be possible to attain absolute sensitivity. A systematic study of fundamental aspects with concomitant theoretical and experimental data might contribute significantly to establishing the realistic performance limits of nanoscale biosensors.

From an application perspective, there is considerable interest in the deployment of such sensors as practical diagnostic tools. The current trend in the area of medical diagnostics aims at bringing the various analytical protocols closer to the point-of-care.[143,191] In general, for the sensitive detection of biomolecules, a broad range of protocols is already available.[14,192] Many of the current assays utilize a multitude of steps and elaborate chemistries in order to achieve this sensitivity. These aspects have been hampering the possibility to realize portable systems for point-of-care diagnostics. Nevertheless, a number of works have been reported where integrated systems with detection stages and complete chemical processing stages have been utilized.[193,194] Simplifying the processing stages is expected to provide a push to the current activities on such point-of-care diagnostic systems. Label-free electrical detection methods based on CNSs can be advantageous for the realization of such systems, since they require very few processing steps. In the ideal case, the sensing device needs to be just exposed to the test solution or the physiological fluid to be analyzed. An added advantage is the low limit of detection achievable. Due to these aspects, CNT- and graphene-based label-free biosensors appear promising for the realization of portable diagnostic systems at the point-of-care or point-of-use.[117,191,195] It is expected that engineered optimized systems based on CNSs may attain a high market value in the coming years.

A number of hurdles remain before such dreams can be realized. The first and foremost obstacle concerns the reproducible fabrication of such sensing devices in a large scale.[15] While there are many examples of large-scale graphene-based devices, realizing CNT-based devices with near-to-identical field-effect characteristics on a wafer scale is still a challenge to be overcome, especially before portable sensors become a reality. A fundamental hurdle for the deployment of such sensors in a realistic scenario is the difficulty in the calibration of these sensors. Until now, most of the sensors have been demonstrated only on a research laboratory scale. For field-use especially in the case of disposable sensors, it is compulsory that they are calibrated and that each sensor provides a well-defined response. In order to achieve this it is necessary to understand the mechanisms of the sensor response in an elaborate manner.[140,196] Once such mechanistic issues are clarified, the design of a portable reader is straightforward. Since only electrical signals are involved, a reader similar to glucometers can be easily conceived. Another important challenge is the possibility to detect a multitude of analytes (multiplex detection) using an array of CNS devices. While this has been widely demonstrated using SiNW devices,[168] very few examples are available based on CNSs.[96] Multiplex detection is particularly attractive in a medical diagnostic scenario, where more than one analyte species may serve as biomarkers for a single disease state. In addition to the challenges mentioned above, the non-availability of CNS devices with identical device characteristics has been a major hurdle in attaining multiplex detection. Other issues that are critical for the widespread application of CNS include reproducibility, stability and the reduction of drift.[186,197] Almost all of the reported sensors have been demonstrated with test solutions. For realistic applications, it is necessary to optimize the protocols in a complex matrix such as blood or serum.[195] Once such engineering aspects are systematically addressed it can be expected that CNSs will open new avenues in the sensitive detection of biomolecules in physiological fluids.

6. Conclusions

In this review, we have presented the state-of-the-art and discussed the challenges in the label-free electrical detection of biomolecules using devices based on carbon nanostructures. Nanobiosensors based on carbon are able to attain high sensitivity with ultralow detection limits, while simultaneously ensuring a good selectivity through controlled chemical functionalization. Moreover, carbon nanotube sensors are able to resolve chemical interactions occurring around individual biomolecules. Despite this progress, very few works have discussed fundamental aspects such as the kinetics of binding, mass transport limitations etc. More systematic investigations both from theoretical and experimental side are necessary to evaluate the real performance limits under practical conditions. An important challenge from an application perspective includes the controlled engineering and optimization of such devices for routine biodetection, where the research is still in its infancy. Once such hurdles are overcome, it can be expected that the various advantages of carbon nanostructures can be synergistically exploited to realize real-life sensors with important applications in fundamental molecular biology and medical diagnostics.

Acknowledgements

This article is part of an ongoing series celebrating the 25th anniversary of *Advanced Materials*.

Received: October 2, 2013
Revised: October 25, 2013
Published online: January 22, 2014

[1] M. Terrones, A. R. Botello-Mendez, J. Campos-Delgado, F. Lopez-Urias, Y. I. Vega-Cantu, F. J. Rodriguez-Macias, A. L. Elias, E. Munoz-Sandoval, A. G. Cano-Marquez, J. C. Charlier, H. Terrones, *Nano Today* **2010**, *5*, 351–372.
[2] D. Vollath, *Nanomaterials: An introduction to synthesis, properties and applications*, Wiley, New York **2013**.
[3] S. K. Pati, T. Enoki, C. N. R. Rao, *Graphene and its fascinating attributes*, World Scientific, Singapore **2011**.

[4] C. N. R. Rao, A. Govindaraj, *Nanotubes and Nanowires*, RSC Publishing, Cambridge, UK **2011**; Vol. 1.
[5] F. L. La Puente, J.-F. Nierengarten, *Fullerenes: Principles and Applications*, 2nd ed., RSC Publishing, Cambridge **2012**.
[6] A. K. Wanekaya, W. Chen, N. V. Myung, A. Mulchandani, *Electroanalysis* **2006**, *18*, 533–550.
[7] S. Liu, X. F. Guo, *NPG Asia Mater* **2012**, *4*, 1–10.
[8] T. Kurkina, K. Balasubramanian, *Cell. Mol. Life Sci.* **2012**, *69*, 373–388.
[9] A. M. Campbell, L. J. Heyer, *Discovering Genomics, Proteomics and Bioinformatics*, Benjamin Cummings, UK **2006**.
[10] V. S. Vaidya, J. V. Bonventre, *Biomarkers: In Medicine, Drug Discovery, and Environmental Health*, Wiley, New Jersey **2010**.
[11] D. Erickson, S. Mandal, A. H. Yang, B. Cordovez, *Microfluidics Nanofluidics* **2008**, *4*, 33–52.
[12] K. B. Mullis, F. Ferre, R. A. Gibbs, *The Polymerase Chain Reaction*, Birkhaeuser, Boston **1994**.
[13] D. A. Giljohann, C. A. Mirkin, *Nature* **2009**, *462*, 461–464.
[14] B. A. White, *PCR Protocols: Current Methods and Applications*, Humana, New Jersey **1993**.
[15] S. Roy, Z. Gao, *Nano Today* **2009**, *4*, 318–334.
[16] K. Balasubramanian, *Biosens. Bioelectron.* **2010**, *26*, 1195–1204.
[17] K. Balasubramanian, M. Burghard, *Small* **2005**, *1*, 180–192.
[18] P. M. Ajayan, M. Terrones, A. de la Guardia, V. Huc, N. Grobert, B. Q. Wei, H. Lezec, G. Ramanath, T. W. Ebbesen, *Science* **2002**, *296*, 705.
[19] T. Guo, P. Nikolaev, A. Thess, D. T. Colbert, R. E. Smalley, *Chem. Phys. Lett.* **1995**, *243*, 49–54.
[20] M. Terrones, N. Grobert, J. Olivares, J. P. Zhang, H. Terrones, K. Kordatos, W. K. Hsu, J. P. Hare, P. D. Townsend, K. Prassides, A. K. Cheetham, H. W. Kroto, D. R. M. Walton, *Nature* **1997**, *388*, 52–55.
[21] M. J. Bronikowski, P. A. Willis, D. T. Colbert, K. A. Smith, R. E. Smalley, *J. Vac. Sci. Technol.* **2001**, *19*, 1800–1805.
[22] M. C. Hersam, *Nat. Nanotechnol.* **2008**, *3*, 387–394.
[23] R. Saito, G. Dresselhaus, M. S. Dresselhaus, *Physical Properties of Carbon Nanotubes*, Imperial College Press, London **1998**.
[24] H. Kataura, Y. Kumazawa, Y. Maniwa, I. Umezu, S. Suzuki, Y. Ohtsuka, Y. Achiba, *Synth. Met.* **1999**, *103*, 2555–2558.
[25] NanoIntegris http://www.nanointegris.com/. (accessed 21 July **2013**).
[26] J. Kong, H. T. Soh, A. M. Cassell, C. F. Quate, H. Dai, *Nature* **1998**, *395*, 878–881.
[27] H. T. Soh, C. F. Quate, A. F. Morpurgo, C. M. Marcus, J. Kong, H. Dai, *Appl. Phys. Lett.* **1999**, *75*, 627–629.
[28] H. J. Dai, *Surf. Sci.* **2002**, *500*, 218–241.
[29] L. Rispal, U. Schwalke, *IEEE Electron Device Lett.* **2008**, *29*, 1349–1352.
[30] S. J. Tans, A. R. M. Verschueren, C. Dekker, *Nature* **1998**, *393*, 49–52.
[31] R. Martel, T. Schmidt, H. R. Shea, T. Hertel, P. Avouris, *Appl. Phys. Lett.* **1998**, *73*, 2447–2449.
[32] J. Kong, N. R. Franklin, C. W. Zhou, M. G. Chapline, S. Peng, K. J. Cho, H. J. Dai, *Science* **2000**, *287*, 622–625.
[33] M. T. Martinez, Y. C. Tseng, N. Ormategui, I. Loinaz, R. Eritja, J. Bokor, *Nano Lett.* **2009**, *9*, 530–536.
[34] R. Krupke, F. Hennrich, H. B. Weber, M. M. Kappes, H. von Lohneysen, *Nano Lett.* **2003**, *3*, 1019–1023.
[35] K. Balasubramanian, T. Kurkina, A. Ahmad, M. Burghard, K. Kern, *J. Mater. Res.* **2012**, *27*, 391–402.
[36] S. Park, R. S. Ruoff, *Nat. Nanotechnol.* **2009**, *4*, 217–224.
[37] C. Mattevi, H. Kim, M. Chhowalla, *J. Mater. Chem.* **2011**, *21*, 3324–3334.
[38] K. S. Novoselov, A. K. Geim, S. V. Morozov, D. Jiang, Y. Zhang, S. V. Dubonos, I. V. Grigorieva, A. A. Firsov, *Science* **2004**, *306*, 666–669.
[39] A. K. Geim, K. S. Novoselov, *Nat. Mater.* **2007**, *6*, 183–191.
[40] R. S. Robinson, K. Sternitzke, M. T. Mcdermott, R. L. Mccreery, *J. Electrochem. Soc.* **1991**, *138*, 2412–2418.
[41] K. I. Bolotin, K. J. Sikes, Z. Jiang, M. Klima, G. Fudenberg, J. Hone, P. Kim, H. L. Stormer, *Solid State Commun.* **2008**, *146*, 351–355.
[42] C. R. Dean, A. F. Young, I. Meric, C. Lee, L. Wang, S. Sorgenfrei, K. Watanabe, T. Taniguchi, P. Kim, K. L. Shepard, J. Hone, *Nat. Nanotechnol.* **2010**, *5*, 722–726.
[43] F. Schedin, A. K. Geim, S. V. Morozov, E. W. Hill, P. Blake, M. I. Katsnelson, K. S. Novoselov, *Nat. Mater.* **2007**, *6*, 652–655.
[44] Y. Hernandez, V. Nicolosi, M. Lotya, F. M. Blighe, Z. Y. Sun, S. De, I. T. McGovern, B. Holland, M. Byrne, Y. K. Gun'ko, J. J. Boland, P. Niraj, G. Duesberg, S. Krishnamurthy, R. Goodhue, J. Hutchison, V. Scardaci, A. C. Ferrari, J. N. Coleman, *Nat. Nanotechnol.* **2008**, *3*, 563–568.
[45] M. Lotya, P. J. King, U. Khan, S. De, J. N. Coleman, *ACS Nano* **2010**, *4*, 3155–3162.
[46] W. S. Hummers, R. E. Offeman, *J. Am. Chem. Soc.* **1958**, *80*, 1339–1339.
[47] C. Gomez-Navarro, R. T. Weitz, A. M. Bittner, M. Scolari, A. Mews, M. Burghard, K. Kern, *Nano Lett.* **2007**, *7*, 3499–3503.
[48] W. W. Cai, R. D. Piner, F. J. Stadermann, S. Park, M. A. Shaibat, Y. Ishii, D. X. Yang, A. Velamakanni, S. J. An, M. Stoller, J. H. An, D. M. Chen, R. S. Ruoff, *Science* **2008**, *321*, 1815–1817.
[49] D. Yang, A. Velamakanni, G. Bozoklu, S. Park, M. Stoller, R. D. Piner, S. Stankovich, I. Jung, D. A. Field, C. A. Ventrice, R. S. Ruoff, *Carbon* **2009**, *47*, 145–152.
[50] D. R. Dreyer, S. Park, C. W. Bielawski, R. S. Ruoff, *Chem. Soc. Rev.* **2010**, *39*, 228–240.
[51] J. Kauppila, P. Kunnas, P. Damlin, A. Viinikanoja, C. Kvarnstrom, *Electrochim. Acta* **2013**, *89*, 84–89.
[52] C. Gomez-Navarro, J. C. Meyer, R. S. Sundaram, A. Chuvilin, S. Kurasch, M. Burghard, K. Kern, U. Kaiser, *Nano Lett.* **2010**, *10*, 1144–1148.
[53] T. Kurkina, S. Sundaram, R. S. Sundaram, F. Re, M. Masserini, K. Kern, K. Balasubramanian, *ACS Nano* **2012**, *6*, 5514–5520.
[54] N. Mohanty, V. Berry, *Nano Lett.* **2008**, *8*, 4469–4476.
[55] R. Stine, J. T. Robinson, P. E. Sheehan, C. R. Tamanaha, *Adv. Mater.* **2010**, *22*, 5297–5300.
[56] S. Myung, A. Solanki, C. Kim, J. Park, K. S. Kim, K. B. Lee, *Adv. Mater.* **2011**, *23*, 2221.
[57] R. Stine, S. P. Mulvaney, J. T. Robinson, C. R. Tamanaha, P. E. Sheehan, *Anal. Chem.* **2012**, *85*, 509–521.
[58] M. Batzill, *Surf. Sci. Rep.* **2012**, *67*, 83–115.
[59] L. Colombo, R. M. Wallace, R. S. Ruoff, *Proc. IEEE* **2013**, *101*, 1536–1556.
[60] E. V. Iski, E. N. Yitamben, L. Gao, N. P. Guisinger, *Adv. Funct. Mater.* **2013**, *23*, 2554–2564.
[61] R. Hawaldar, P. Merino, M. R. Correia, I. Bdikin, J. Gracio, J. Mendez, J. A. Martin-Gago, M. K. Singh, *Sci. Rep.* **2012**, *2*.
[62] P. Y. Huang, C. S. Ruiz-Vargas, A. M. van der Zande, W. S. Whitney, M. P. Levendorf, J. W. Kevek, S. Garg, J. S. Alden, C. J. Hustedt, Y. Zhu, J. Park, P. L. McEuen, D. A. Muller, *Nature* **2011**, *469*, 389.
[63] W. Gannett, W. Regan, K. Watanabe, T. Taniguchi, M. F. Crommie, A. Zettl, *Appl. Phys. Lett.* **2011**, *98*.
[64] I. Meric, C. R. Dean, N. Petrone, L. Wang, J. Hone, P. Kim, K. L. Shepard, *Proc. IEEE* **2013**, *101*, 1609–1619.
[65] X. S. Li, W. W. Cai, J. H. An, S. Kim, J. Nah, D. X. Yang, R. Piner, A. Velamakanni, I. Jung, E. Tutuc, S. K. Banerjee, L. Colombo, R. S. Ruoff, *Science* **2009**, *324*, 1312–1314.
[66] S. J. Kang, B. Kim, K. S. Kim, Y. Zhao, Z. Y. Chen, G. H. Lee, J. Hone, P. Kim, C. Nuckolls, *Adv. Mater.* **2011**, *23*, 3531.
[67] J. Song, F. Y. Kam, R. Q. Png, W. L. Seah, J. M. Zhuo, G. K. Lim, P. K. H. Ho, L. L. Chua, *Nat. Nanotechnol.* **2013**, *8*, 356–362.
[68] M. Burghard, H. Klauk, K. Kern, *Adv. Mater.* **2009**, *21*, 2586–2600.

[69] P. Avouris, F. N. Xia, *MRS Bulletin* **2012**, *37*, 1225–1234.
[70] D. Jariwala, V. K. Sangwan, L. J. Lauhon, T. J. Marks, M. C. Hersam, *Chem. Soc. Rev.* **2013**, *42*, 2824–2860.
[71] F. Schwierz, *Nat Nano* **2010**, *5*, 487–496.
[72] A. Jorio, M. S. Dresselhaus, G. Dresselhaus, *Carbon Nanotubes: Advanced Topics in the Synthesis, Structure, Properties and Applications*, Springer, Berlin Heidelberg, **2008**.
[73] I. Heller, S. Chatoor, J. Mannik, M. A. G. Zevenbergen, C. Dekker, S. G. Lemay, *J. Am. Chem. Soc.* **2010**, *132*, 17149–17156.
[74] K. Balasubramanian, E. J. H. Lee, R. T. Weitz, M. Burghard, K. Kern, *Phy. Status Solidi A* **2008**, *205*, 633–646.
[75] J. L. Xia, F. Chen, J. H. Li, N. J. Tao, *Nat. Nanotechnol.* **2009**, *4*, 505–509.
[76] T. Fang, A. Konar, H. Xing, D. Jena, *Appl. Phys. Lett.* **2007**, *91*, 092109–3.
[77] D. Wei, M. J. A. Bailey, P. Andrew, T. Ryhanen, *Lab Chip* **2009**, *9*, 2123–2131.
[78] E. J. H. Lee, K. Balasubramanian, R. T. Weitz, M. Burghard, K. Kern, *Nat. Nanotechnol.* **2008**, *3*, 486–490.
[79] T. Enoki, Y. Kobayashi, K. I. Fukui, *Int. Rev. Phys. Chem.* **2007**, *26*, 609–645.
[80] R. S. Sundaram, C. Gomez-Navarro, K. Balasubramanian, M. Burghard, K. Kern, *Adv. Mater.* **2008**, *20*, 3050–3053.
[81] H. Vedala, D. C. Sorescu, G. P. Kotchey, A. Star, *Nano Lett.* **2011**, *11*, 2342–2347.
[82] S. Ryu, M. Y. Han, J. Maultzsch, T. F. Heinz, P. Kim, M. L. Steigerwald, L. E. Brus, *Nano Lett.* **2008**, *8*, 4597–4602.
[83] J. L. Bahr, J. M. Tour, *J. Mater. Chem.* **2002**, *12*, 1952–1958.
[84] L. Rodriguez-Perez, M. A. Herranz, N. Martin, *Chem. Commun. (Cambridge, U. K.)* **2013**, *49*, 3721–3735.
[85] X. F. Gao, Y. Wang, X. Liu, T. L. Chan, S. Irle, Y. L. Zhao, S. B. B. Zhang, *Phys. Chem. Chem. Phys.* **2011**, *13*, 19449–19453.
[86] X. Peng, S. S. Wong, *Adv. Mater.* **2009**, *21*, 625–642.
[87] D. A. C. Brownson, D. K. Kampouris, C. E. Banks, *Chem. Soc. Rev.* **2012**, *41*, 6944–6976.
[88] S. C. S. Lai, A. N. Patel, K. McKelvey, P. R. Unwin, *Angew. Chem. Int. Ed.* **2012**, *51*, 5405–5408.
[89] T. Y. Zhai, L. Li, Y. Ma, M. Y. Liao, X. Wang, X. S. Fang, J. N. Yao, Y. Bando, D. Golberg, *Chem. Soc. Rev.* **2011**, *40*, 2986–3004.
[90] T. Y. Zhai, X. S. Fang, M. Y. Liao, X. J. Xu, H. B. Zeng, B. Yoshio, D. Golberg, *Sensors-Basel* **2009**, *9*, 6504–6529.
[91] R. M. Penner, *Annu. Rev. Anal. Chem.* **2012**, *5*, 461–485.
[92] G. J. Zhang, Y. Ning, *Anal. Chim. Acta* **2012**, *749*, 1–15.
[93] F. Patolsky, G. Zheng, C. M. Lieber, *Nat. Protocols* **2006**, *1*, 1711–24.
[94] Z. Q. Gao, A. Agarwal, A. D. Trigg, N. Singh, C. Fang, C. H. Tung, Y. Fan, K. D. Buddharaju, J. M. Kong, *Anal. Chem.* **2007**, *79*, 3291–3297.
[95] E. Stern, A. Vacic, N. K. Rajan, J. M. Criscione, J. Park, B. R. Ilic, D. J. Mooney, M. A. Reed, T. M. Fahmy, *Nat. Nanotechnol.* **2010**, *5*, 138–142.
[96] Q. F. Pengfei, O. Vermesh, M. Grecu, A. Javey, O. Wang, H. J. Dai, S. Peng, K. J. Cho, *Nano Lett.* **2003**, *3*, 347–351.
[97] B. R. Li, C. W. Chen, W. L. Yang, T. Y. Lin, C. Y. Pan, Y. T. Chen, *Biosens. Bioelectron.* **2013**, *45*, 252–259.
[98] Y. L. Bunimovich, Y. S. Shin, W. S. Yeo, M. Amori, G. Kwong, J. R. Heath, *J. Am. Chem. Soc.* **2006**, *128*, 16323–16331.
[99] W. Kim, A. Javey, O. Vermesh, Q. Wang, Y. Li, H. Dai, *Nano Lett.* **2003**, *3*, 193–198.
[100] P. Bergveld, *Sens. Actuators, B* **2003**, *88*, 1–20.
[101] A. Poghossian, A. Cherstvy, S. Ingebrandt, A. Offenhausser, M. J. Schoning, *Sens. Actuators B* **2005**, *111*, 470–480.
[102] E. D. Minot, A. M. Janssens, I. Heller, H. A. Heering, C. Dekker, S. G. Lemay, *Appl. Phys. Lett.* **2007**, *91*.
[103] I. Heller, S. Chatoor, J. Mannik, M. A. G. Zevenbergen, C. Dekker, S. G. Lemay, *Phys. Status Solidi RRL* **2009**, *3*, 190–192.
[104] S. Rosenblatt, Y. Yaish, J. Park, J. Gore, V. Sazonova, P. L. McEuen, *Nano Lett.* **2002**, *2*, 869–872.
[105] R. S. Sundaram, M. Steiner, H.-Y. Chiu, M. Engel, A. A. Bol, R. Krupke, M. Burghard, K. Kern, P. Avouris, *Nano Lett.* **2011**, *11*, 3833–3837.
[106] S. Heinze, J. Tersoff, R. Martel, V. Derycke, J. Appenzeller, P. Avouris, *Phys. Rev. Lett.* **2002**, *89*, 106801.
[107] A. Maroto, K. Balasubramanian, M. Burghard, K. Kern, *ChemPhysChem* **2007**, *8*, 220–223.
[108] A. Star, E. Tu, J. Niemann, J. C. P. Gabriel, C. S. Joiner, C. Valcke, *Proc. Natl. Acad. Sci. USA* **2006**, *103*, 921–926.
[109] T. Kurkina, A. Vlandas, A. Ahmad, K. Kern, K. Balasubramanian, *Angew. Chem. Int. Ed.* **2011**, *50*, 3710–3714.
[110] M. Dankerl, M. V. Hauf, A. Lippert, L. H. Hess, S. Birner, I. D. Sharp, A. Mahmood, P. Mallet, J. Y. Veuillen, M. Stutzmann, J. A. Garrido, *Adv. Funct. Mater.* **2010**, *20*, 3117–3124.
[111] C. T. Lin, P. T. K. Loan, T. Y. Chen, K. K. Liu, C. H. Chen, K. H. Wei, L. J. Li, *Adv. Funct. Mater.* **2013**, *23*, 2301–2307.
[112] A. Bonanni, A. H. Loo, M. Pumera, *TrAC, Trends Anal. Chem.* **2012**, *37*, 12–21.
[113] A. Kanwal, S. Lakshmanan, A. Bendiganavale, C. T. Bot, A. Patlolla, R. Raj, C. Prodan, Z. Iqbal, G. A. Thomas, R. C. Farrow, *Biosens. Bioelectron.* **2013**, *45*, 267–273.
[114] K. Balasubramanian, M. Burghard, *Anal. Bioanal. Chem.* **2006**, *385*, 452–468.
[115] J. P. Lei, H. X. Ju, *Wiley. Interdiscip. Rev.: Nanomed. Nanobiotechnol.* **2010**, *2*, 496–509.
[116] S. Kochmann, T. Hirsch, O. S. Wolfbeis, *TrAC, Trends Anal. Chem.* **2012**, *39*, 87–113.
[117] B. Perez-Lopez, A. Merkoci, *Microchim. Acta* **2012**, *179*, 1–16.
[118] M. Ali, R. Neumann, W. Ensinger, *ACS Nano* **2010**, *4*, 7267–7274.
[119] R. J. Chen, H. C. Choi, S. Bangsaruntip, E. Yenilmez, X. W. Tang, Q. Wang, Y. L. Chang, H. J. Dai, *J. Am. Chem. Soc.* **2004**, *126*, 1563–1568.
[120] S. Okamoto, Y. Ohno, K. Maehashi, K. Inoue, K. Matsumoto, *Jpn. J. Appl. Phys.* **2012**, *51*.
[121] S. Liu, X. Y. Zhang, W. X. Luo, Z. X. Wang, X. F. Guo, M. L. Steigerwald, X. H. Fang, *Angew. Chem. Int. Ed.* **2011**, *50*, 2496–2502.
[122] A. H. Loo, A. Bonanni, M. Pumera, *Chem-Asian J* **2013**, *8*, 198–203.
[123] K. Besteman, J. O. Lee, F. G. M. Wiertz, H. A. Heering, C. Dekker, *Nano Lett.* **2003**, *3*, 727–730.
[124] A. Vlandas, T. Kurkina, A. Ahmad, K. Kern, K. Balasubramanian, *Anal. Chem.* **2010**, *82*, 6090–6097.
[125] M. Shim, N. W. Shi Kam, R. J. Chen, Y. Li, H. Dai, *Nano Lett.* **2002**, *2*, 285–288.
[126] T. Dastagir, E. S. Forzani, R. Zhang, I. Amlani, L. A. Nagahara, R. Tsui, N. Tao, *Analyst* **2007**, *132*, 738–740.
[127] S. Sorgenfrei, C. Y. Chiu, R. L. Gonzalez, Y. J. Yu, P. Kim, C. Nuckolls, K. L. Shepard, *Nat. Nanotechnol.* **2011**, *6*, 125–131.
[128] K. Balasubramanian, M. Burghard, *J. Mater. Chem.* **2008**, *18*, 3071–3083.
[129] K. Balasubramanian, M. Friedrich, C. Y. Jiang, Y. W. Fan, A. Mews, M. Burghard, K. Kern, *Adv. Mater.* **2003**, *15*, 1515–1518.
[130] K. Balasubramanian, M. Burghard, K. Kern, *Phys. Chem. Chem. Phys.* **2008**, *10*, 2256–2262.
[131] M. Burghard, A. Maroto, K. Balasubramanian, T. Assmus, A. Forment-Aliaga, E. J. H. Lee, R. T. Weitz, M. Scolari, F. Nan, A. Mews, K. Kern, *Phys. Status Solidi B* **2007**, *244*, 4021–4025.
[132] W. T. Mook, M. K. Aroua, M. H. Chakrabarti, C. T. J. Low, P. V. Aravind, N. P. Brandon, *Electrochim. Acta* **2013**, *94*, 327–335.

[133] E. Stern, R. Wagner, F. J. Sigworth, R. Breaker, T. M. Fahmy, M. A. Reed, *Nano Lett.* **2007**, *7*, 3405–3409.
[134] J. P. Lukaszewicz, *Sens. Lett.* **2006**, *4*, 53–98.
[135] S. Liu, Q. Shen, Y. Cao, L. Gan, Z. X. Wang, M. L. Steigerwald, X. F. Guo, *Coord. Chem. Rev.* **2010**, *254*, 1101–1116.
[136] C. Gao, Z. Guo, J. H. Liu, X. J. Huang, *Nanoscale* **2012**, *4*, 1948–1963.
[137] D. W. Boukhvalov, M. I. Katsnelson, *J. Phys.: Condens. Matter* **2009**, *21*.
[138] T. Kuila, S. Bose, A. K. Mishra, P. Khanra, N. H. Kim, J. H. Lee, *Prog. Mater. Sci.* **2012**, *57*, 1061–1105.
[139] Q. Tang, Z. Zhou, Z. F. Chen, *Nanoscale* **2013**, *5*, 4541–4583.
[140] I. Heller, A. M. Janssens, J. Mannik, E. D. Minot, S. G. Lemay, C. Dekker, *Nano Lett.* **2008**, *8*, 591–595.
[141] K. Balasubramanian, M. Burghard, K. Kern, M. Scolari, A. Mews, *Nano Lett.* **2005**, *5*, 507–510.
[142] B. R. Eggins, *Chemical Sensors and Biosensors*, Wiley, Wiltshire, UK, **2002**.
[143] K. Dill, R. Liu, P. Grodzinski, *Microarrays: Preparation, Microfluidics, Detection Methods, and Biological Applications*, Springer, Berlin-Heidelberg **2009**.
[144] X. Tang, S. Bansaruntip, N. Nakayama, E. Yenilmez, Y. L. Chang, Q. Wang, *Nano Lett.* **2006**, *6*, 1632–6.
[145] E. L. Gui, L. J. Li, K. K. Zhang, Y. P. Xu, X. C. Dong, X. N. Ho, P. S. Lee, J. Kasim, Z. X. Shen, J. A. Rogers, S. G. Mhaisalkar, *J. Am. Chem. Soc.* **2007**, *129*, 14427–14432.
[146] Y. K. Baek, S. M. Yoo, J. H. Kim, D. H. Jung, Y. K. Choi, Y. S. Kim, S. Y. Lee, H. T. Jung, *J. Phys. Chem. C* **2009**, *113*, 21566–21571.
[147] X. C. Dong, C. M. Lau, A. Lohani, S. G. Mhaisalkar, J. Kasim, Z. X. Shen, X. N. Ho, J. A. Rogers, L. J. Li, *Adv. Mater.* **2008**, *20*, 2389.
[148] K. Balasubramanian, *Eng. Life Sci.* **2012**, *12*, 121–130.
[149] T. Y. Chen, T. K. L. Phan, C. L. Hsu, Y. H. Lee, J. T. W. Wang, K. H. Wei, C. T. Lin, L. J. Li, *Biosens. Bioelectron.* **2013**, *41*, 103–109.
[150] X. C. Dong, Y. M. Shi, W. Huang, P. Chen, L. J. Li, *Adv. Mater.* **2010**, *22*, 1649.
[151] J. S. Li, Y. L. Zhang, S. To, L. D. You, Y. Sun, *ACS Nano* **2011**, *5*, 6661–6668.
[152] S. Adam, E. H. Hwang, V. M. Galitski, S. Das Sarma, *Proc. Natl. Acad. Sci. USA* **2007**, *104*, 18392–18397.
[153] H. R. Byon, H. C. Choi, *J. Am. Chem. Soc.* **2006**, *128*, 2188–2189.
[154] H. R. Byon, S. Kim, H. C. Choi, *NANO* **2008**, *3*, 415–431.
[155] A. Star, J. C. P. Gabriel, K. Bradley, G. Gruner, *Nano Lett.* **2003**, *3*, 459–463.
[156] C. Li, M. Curreli, H. Lin, B. Lei, F. N. Ishikawa, R. Datar, R. J. Cote, M. E. Thompson, C. W. Zhou, *J. Am. Chem. Soc.* **2005**, *127*, 12484–12485.
[157] K. Maehashi, T. Katsura, K. Kerman, Y. Takamura, K. Matsumoto, E. Tamiya, *Anal. Chem.* **2007**, *79*, 782–787.
[158] H. M. So, K. Won, Y. H. Kim, B. K. Kim, B. H. Ryu, P. S. Na, H. Kim, J. O. Lee, *J. Am. Chem. Soc.* **2005**, *127*, 11906–11907.
[159] T. Nguyen, J. P. Hilton, Q. Lin, *Microfluidics Nanofluidics* **2009**, *6*, 347–362.
[160] E. Engvall, P. Perlmann, *Immunochemistry* **1971**, *8*, 871.
[161] A. K. Feldman, M. L. Steigerwald, X. F. Guo, C. Nuckolls, *Acc. Chem. Res.* **2008**, *41*, 1731–1741.
[162] Y. Ohno, K. Maehashi, K. Matsumoto, *J. Am. Chem. Soc.* **2010**, *132*, 18012–18013.
[163] S. Mao, G. H. Lu, K. H. Yu, Z. Bo, J. H. Chen, *Adv. Mater.* **2010**, *22*, 3521.
[164] J. Hardy, D. J. Selkoe, *Science* **2002**, *297*, 353–6.
[165] E. Cazzaniga, A. Bulbarelli, E. Lonati, A. Orlando, F. Re, M. Gregori, M. Masserini, *Neurochem. Res.* **2011**, *36*, 863–869.
[166] Y. Cui, Q. Q. Wei, H. K. Park, C. M. Lieber, *Science* **2001**, *293*, 1289–1292.
[167] E. Stern, J. F. Klemic, D. A. Routenberg, P. N. Wyrembak, D. B. Turner-Evans, A. D. Hamilton, D. A. LaVan, T. M. Fahmy, M. A. Reed, *Nature* **2007**, *445*, 519–522.
[168] G. Zheng, F. Patolsky, Y. Cui, W. U. Wang, C. M. Lieber, *Nat. Biotechnol.* **2005**, *23*, 1294–1301.
[169] A. Kim, C. S. Ah, H. Y. Yu, J. H. Yang, I. B. Baek, C. G. Ahn, C. W. Park, M. S. Jun, S. Lee, *Appl. Phys. Lett.* **2007**, *91*.
[170] L. H. Hess, M. Jansen, V. Maybeck, M. V. Hauf, M. Seifert, M. Stutzmann, I. D. Sharp, A. Offenhausser, J. A. Garrido, *Adv. Mater.* **2011**, *23*, 5045–5049.
[171] Y. X. Huang, X. C. Dong, Y. X. Liu, L. J. Li, P. Chen, *J. Mater. Chem.* **2011**, *21*, 12358–12362.
[172] H. M. So, D. W. Park, E. K. Jeon, Y. H. Kim, B. S. Kim, C. K. Lee, S. Y. Choi, S. C. Kim, H. Chang, J. O. Lee, *Small* **2008**, *4*, 197–201.
[173] R. A. Villamizar, A. Maroto, F. X. Rius, I. Inza, M. J. Figueras, *Biosens. Bioelectron.* **2008**, *24*, 279–283.
[174] Y. Choi, I. S. Moody, P. C. Sims, S. R. Hunt, B. L. Corso, I. Perez, G. A. Weiss, P. G. Collins, *Science* **2012**, *335*, 319–324.
[175] Y. Choi, T. J. Olsen, P. C. Sims, I. S. Moody, B. L. Corso, M. N. Dang, G. A. Weiss, P. G. Collins, *Nano Lett.* **2013**, *13*, 625–631.
[176] Y. Choi, I. S. Moody, P. C. Sims, S. R. Hunt, B. L. Corso, D. E. Seitz, L. C. Blaszczak, P. G. Collins, G. A. Weiss, *J. Am. Chem. Soc.* **2012**, *134*, 8286–8286.
[177] J. R. Lakowicz, *Principles of Fluorescence Spectroscopy*, 3rd ed.; Springer, Heidelberg, **2006**.
[178] V. I. Claessen, H. Engelkamp, P. C. M. Christianen, J. C. Maan, R. J. M. Nolte, K. Blank, A. E. Rowan, *Annu. Rev. Anal. Chem.* **2010**, *3*, 319–340.
[179] M. A. G. Zevenbergen, P. S. Singh, E. D. Goluch, B. L. Wolfrum, S. G. Lemay, *Anal. Chem.* **2009**, *81*, 8203–8212.
[180] H. P. Lu, L. Xun, X. S. Xie, *Science* **1998**, *282*, 1877–1882.
[181] S. Birner, C. Uhl, M. Bayer, P. Vogl, *Physics-Based Mathematical Models for Low-Dimensional Semiconductor Nanostructures: Analysis and Computation* **2008**, *107*.
[182] R. B. Schasfoort, A. J. Tudos, *Handbook of Surface Plasmon Resonance*, RSC Publishing, Cambridge, UK, **2008**.
[183] C. J. Shih, Q. H. Wang, Z. Jin, G. L. C. Paulus, D. Blankschtein, P. Jarillo-Herrero, M. S. Strano, *Nano Lett.* **2013**, *13*, 809–817.
[184] R. Stine, S. P. Mulvaney, J. T. Robinson, C. R. Tamanaha, P. E. Sheehan, *Anal. Chem.* **2013**, *85*, 509–521.
[185] A. B. Dahlin, *Sensors-Basel* **2012**, *12*, 3018–3036.
[186] T. M. Squires, R. J. Messinger, S. R. Manalis, *Nat. Biotechnol.* **2008**, *26*, 417–426.
[187] P. E. Sheehan, L. J. Whitman, *Nano Lett.* **2005**, *5*, 803–807.
[188] I. Heller, J. Kong, K. A. Williams, C. Dekker, S. G. Lemay, *J. Am. Chem. Soc.* **2006**, *128*, 7353–7359.
[189] J. Go, M. A. Alam, *Appl. Phys. Lett.* **2009**, *95*, 033110–3.
[190] P. R. Nair, M. A. Alam, *Appl. Phys. Lett.* **2006**, *88*, 233120–3.
[191] C. I. L. Justino, T. A. P. Rocha-Santos, A. C. Duarte, *TrAC, Trends Anal. Chem.* **2013**, *45*, 24–36.
[192] M. Schena, *Protein Microarrays*, Jones & Bartlett, New York **2004**.
[193] X. L. Xu, S. Zhang, H. Chen, J. L. Kong, *Talanta* **2009**, *80*, 8–18.
[194] R. H. Liu, J. N. Yang, R. Lenigk, J. Bonanno, P. Grodzinski, *Anal. Chem.* **2004**, *76*, 1824–1831.
[195] M. S. Makowski, A. Ivanisevic, *Small* **2011**, *7*, 1863–1875.
[196] B. K. Wunderlich, P. A. Neff, A. R. Bausch, *Appl. Phys. Lett.* **2007**, *91*.
[197] S. S. Karajanagi, A. A. Vertegel, R. S. Kane, J. S. Dordick, *Langmuir* **2004**, *20*, 11594–11599.

Materials Science

Top Journals and their 2012 Impact Factors*

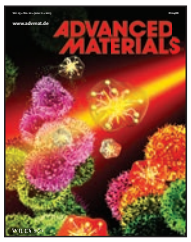

App to be launched soon!

Advanced Materials

Impact Factor: 14.829
One key to the success of *Advanced Materials* is its pronounced interdisciplinary, manifested in its rare listing in six different subject categories. It is ranked #1 with 91,952 citations in Nanoscience & Nanotechnology and ranked #2 in Multidisciplinary Materials Science.

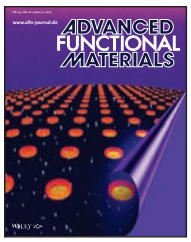

Advanced Functional Materials

Impact Factor: 9.765
Advanced Functional Materials reinforces its standing as a leading full-paper general materials science journal.

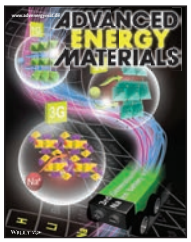

Advanced Energy Materials

First Impact Factor: 10.043
Advanced Energy Materials received its first Impact Factor of 10.043. It confirms in numbers that *Advanced Energy Materials* has joined *Advanced Materials*, *Advanced Functional Materials* and *Small* as top quality journal, publishing in the field of energy-related research.

Small

Impact Factor: 7.823
With an Impact Factor of 7.823, *Small* continues to be the premier journal for research at the nano- and mircoscale.

Particle

Impact Factor: 0.857
Particle, a member of the *Advanced* journals family, focuses on all aspects of particle research.
It is one of the top 10 journals in Characterization & Testing by Impact Factor and by total citations, too.

Macromolecular Bioscience

Impact Factor: 3.742
Macromolecular Bioscience is ranked among the top 5 biomaterials journals and listed among the top 10 polymer journals. It maintains its position as the leading journal at the intersection of materials and polymer science with life sciences and medicine.

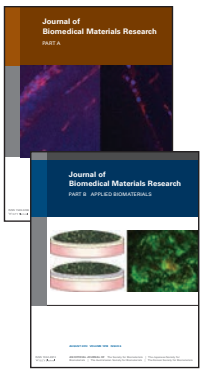

Journal of Biomedical Materials Research, Part A

Impact Factor: 2.834
It is ranked #2 with 12,128 citations in Biomaterials.
Published on behalf of the *Society for Biomaterials*.

Journal of Biomedical Materials Research, Part B

Impact Factor: 2.308
Published on behalf of the *Society for Biomaterials*.

Journal of the American Ceramic Society

Impact Factor: 2.107
The journal continues to far outpace all other Ceramic related journals with over 30,500 total cites!
Published on behalf of the *The American Ceramic Society*.

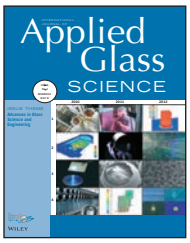

International Journal of Applied Glass Science

First Impact Factor: 1.548
The journal received its first Impact Factor of 1.548 and has established itself as an indispensable source of knowledge on the application of glass science and engineering across the entire materials spectrum.
Published on behalf of *The American Ceramic Society*.

NEW JOURNALS

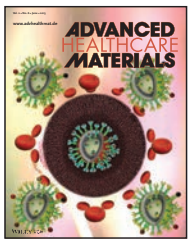

Advanced Healthcare Materials

First Immediacy Index: 0.712
Launched in 2012, *Advanced Healthcare Materials* received its first Immediacy Index of 0.712. This inaugural value establishes *Advanced Healthcare Materials* as a premier journal for publishing biomedical materials research.
www.advhealthmat.com

Get complimentary online access in 2013:
wileyonlinelibrary.com/newjournals-optin

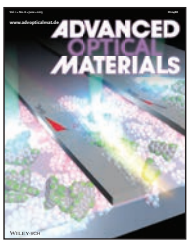

Advanced Optical Materials

First Immediacy Index will be announced in 2014.
This new journal was founded in 2013 as a member of the *Advanced* journals family.
It is covering all aspects of light-matter interactions, including topics like plasmonics, metamaterials, photonics and more.
www.advopticalmat.com

Get complimentary online access in 2013&2014:
wileyonlinelibrary.com/newjournals-optin

wileyonlinelibrary.com/subject/materials

*2013 Release of Journal Citation Reports®
Source: Thomson Reuters 2012 Citation Data

WILEY

13-57244